AD-A143 917 DIGITAL CONTROL OF FLIGHT SIMULATOR MOTION BASE ACTUATOR(U) AERONAUTICAL RESEARCH LABS MELBOURNE (AUSTRALIA) J SANDOR JAN 84 ARL/SYS-TM-69 1/1

UNCLASSIFIED F/G 5/9 NL

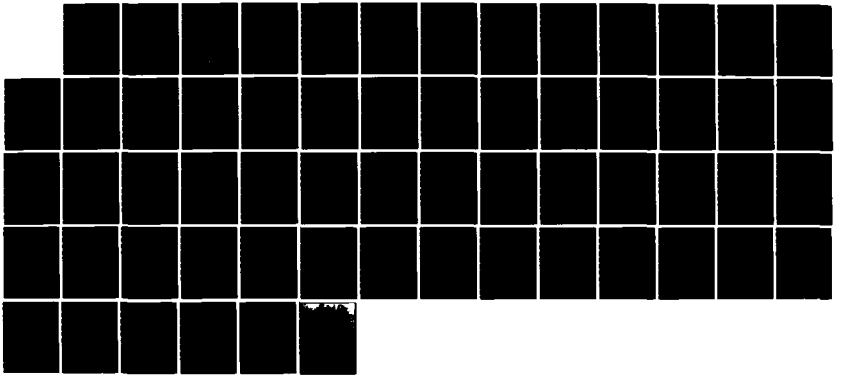

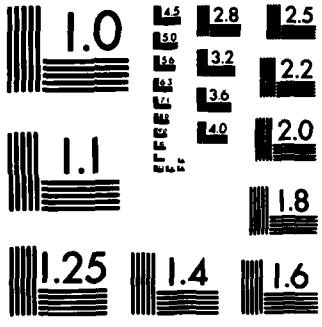

MICROCOPY RESOLUTION TEST CHART
NATIONAL BUREAU OF STANDARDS-1963-A

(12)

AHL- SYS-TM-69

AR-003-006

AUSTRALIA

AD-A143 917

DEPARTMENT OF DEFENCE

ENCE SCIENCE AND TECHNOLOGY ORGANISATION

AERONAUTICAL RESEARCH LABORATORIES

MELBOURNE, VICTORIA

Systems Technical Memorandum 69

DIGITAL CONTROL OF FLIGHT SIMULATOR MOTION BASE ACTUATOR

J. SANDOR

THE UNITED STATES NATIONAL TECHNICAL INFORMATION SERVICE IS AUTHORISED TO REPRODUCE AND SELL THIS REPORT

Approved for Public Release

DTIC FILE COPY

DTIC ELECTE AUG 21 1984 E

(C) Commenwealth of Australia 1984

JANUARY 1984

COPY No 84

085

AR-003-006

DEPARTMENT OF DEFENCE

DEFENCE SCIENCE AND TECHNOLOGY ORGANISATION

AERONAUTICAL RESEARCH LABORATORIES

Systems Technical Memorandum 69

DIGITAL CONTROL OF FLIGHT SIMULATOR MOTION BASE

by

J. SANDOR

Digital control strategies for a nonlinear motion base actuator are considered and a compound linear/nonlinear algorithm is derived for velocity tracking under a range of load conditions for representative motion demands. Discrete frequency domain methods are employed to synthesize the linear components of the control law and to establish the stability of the closed loop system via describing function analysis. The nonlinear compensation, providing attenuation of Coulomb friction effects, is realised through a velocity dependent gain term, which does not significantly affect the satisfactory large amplitude system response. Overall closed loop system performance is validated through computer simulation.

© COMMONWEALTH OF AUSTRALIA 1984

POSTAL ADDRESS: Director, Aeronautical Research Laboratories,
P.O. Box 4331, Melbourne, Victoria, 3001, Australia.

CONTENTS

		PAGE NO.
NOTATION		
1.	INTRODUCTION	1
2.	SYSTEM MODEL AND PERFORMANCE SPECIFICATION	2
.21	Motion Base Description	2
2.2	Motor/Load Model	4
2.3	Control System Configuration	6
2.4	Performance Specification	6
2.5	Sample Reference Velocity Inputs	9
3.	CONTROL COMPENSATOR SYNTHESIS	9
3.1	Basic Considerations	9
3.2	Digital Control Law	13
3.3	System Stability in the Presence of Static and Sliding Friction	21
4.	SIMULATION OF CLOSED LOOP SYSTEM	35
5.	NONLINEAR COMPENSATION	35
6.	CONCLUDING REMARKS	37
REFERENCES		
APPENDIX - Simulation Results		
DISTRIBUTION LIST		
DOCUMENT CONTROL DATA		

Accession For
NTIS GRA&I
DTIC TAB
Unannounced
Justification
By
Distribution/
Availability Codes
Dist | Avail and/or Special
A-1

DTIC COPY INSPECTED 3

NOTATION

E	motor emf (V)
I	armature current (A)
r_a	armature resistance (ohm)
k_T	motor torque constant (Nm/A)
k_E	motor emf constant (V/rad sec^{-1})
T	motor torque (Nm)
w	motor velocity (rad sec^{-1})
V	applied motor voltage (V)
k_D	damping torque constant (Nm)
T_F	Coulomb friction torque (Nm)
T_S	static friction torque (Nm) (T_F at $w=0$)
T_R	running friction torque (Nm) (T_F at $w\neq 0$)
T_o	available motor torque (Nm)
f	inverse of motor regulation (Nm/rad sec^{-1})
k_s	spring restoring torque rate (Nm/rad)
J	inertia ($kg - m^2$)
Δt	sampling interval (sec)
w_r	velocity reference input (rad sec^{-1})
θ_r	reference input angle (rad)
θ	motor angle (rad)
s	Laplace Transform variable
R_w	r.m.s. velocity response error
$R_{\dot{w}}$	r.m.s. acceleration response error
$\ell\Delta t$	average response delay (sec)
$\Omega_r(s)$	Laplace transform of $w_r(t)$
$\Omega(s)$	Laplace transform of $w(t)$
k_p	proportional gain

.../cont.

NOTATION (CONT.)

k_i	integral gain
$\theta_r(s)$	Laplace transform of $\theta_r(t)$
$\theta(s)$	Laplace transform of $\theta(t)$
ω	Frequency (rad sec^{-1})

1. INTRODUCTION

Motion cue generation is a significant factor is any manned flight simulation facility. Such a facility is being developed at the Aeronautical Research Laboratories in support of research in synthetic training technology and aircraft system studies. A key element of the development work is the formulation of (digital) control strategies for motion base systems to synthesize position, velocity and acceleration in a manner that replicates, most effectively, the cueing environment, subject to the overall excursion and rate constraints intrinsic to the motion base actuators. In support of these aims investigations are being made into the synthesis of tunable control laws for velocity control of actuators under a range of load and reference input conditions in the presence of intrinsic nonlinearities and time delays.

This report describes the derivation of a control algorithm for the electric servomotor drives of a 4 degrees-of-freedom synergistic simulator motion platform. The performance criteria are specified in terms of the error between the reference velocity input and the motor velocity response profile for a range of inertial and spring restoring loads and subject to maximum allowable response time delay. (Here reference input velocity refers to the motion base drive signal and includes washout). In addition to the preceding requirements, control law complexity is constrained to be such that a four channel controller can be realized on a single DEC LSI-11/23 microcomputer operating at 50 Hz sampling rate.

The control law presented comprises a linear proportional plus integral (PI) term with compensation to meet performance and tunability requirements and a nonlinear term to attenuate the transient effects of Coulomb friction. This control regime is derived in three steps: firstly a discrete frequency domain approach, based on a z-transform model of the linearized system, is adopted for the derivation of the linear terms of the controller such that satisfactory stability margins are achieved for the linearized system under the specified load conditions and loop time delays. Secondly, the stability of the nonlinear closed loop system is established by using harmonic linearization for mathematically characterising Coulomb friction and the application of describing function analysis. Finally, based on the simulation of the linearly controlled system, a smooth nonlinear control term is synthesised for the attenuation of friction effects which are shown to be particularly significant for low amplitude reference inputs. The nonlinear control term effects an increase in the system loop gain in regimes where Coulomb friction becomes dominant, without adversely affecting the satisfactory large amplitude response of the linearly controlled system.

In the present case, given the controller complexity constraints and the requirement for tunability, the frequency domain synthesis method is preferred to that of either optimal control theory or deadbeat controller design. The former is based on the minimization of a quadratic penalty function, which here would require the solution of a computationally costly two point boundary value problem [9], whilst the realization of the resulting control algorithm requires estimation of all the system states.

Deadbeat control algorithms, on the other hand require a priori knowledge of system inputs, are not readily tunable, and may require excessive control effort to achieve deadbeat response [4]. In contrast, frequency domain methods offer readily computable, tunable, time-invariant control laws, implementable in recursive form and giving satisfactory response for a range of system inputs and loads. Their principal limitations, apart from non-optimality, is that for nonlinear systems closed loop stability is not a priori guaranteed. However, for the system under consideration here, where the linear parts of the system have low pass frequency characteristics, this difficulty can be overcome by application of describing function analysis.

2. SYSTEM MODEL AND PERFORMANCE SPECIFICATION

2.1 Motion Base Description

The four degrees-of-freedom simulator motion base under consideration comprises a metal, two-man, side by side, cockpit mounted on a pneumatically balanced suspension system with motion actuation derived from 4 direct current printed circuit motors via screw jacks attached to the cockpit. Two motor/screwjack actuators are attached to the rear of the cockpit whilst another pair, inclined to the vertical, are attached through a "knuckle" arrangement to the front of the cockpit as depicted in Figure 2.1. The operation of the motion base is synergistic: that is, it requires a combination of actuator extensions to achieve motion in any one degree of freedom. This "coupling" effect results in varying inertial and spring restoring loads on each motor. For example, heave motion is realized with all four actuators driving the load, which includes the spring restoring force of the suspension system. On the other hand, for yaw, the front actuators drive the load, with the rear actuators only tracking, and the suspension system providing practically no restoring force.

The screw jacks comprise a 25 mm lead screw and a nut with a maximum linear travel of 415 mm for the front jacks and 590 mm for the rear jacks. The maximum cockpit excursion about the central position for each degree of freedom is -

heave : ± 300 mm

pitch : ± 25°

roll : ± 17°

yaw : ± 12°

Each motor is a Yaskawa printed circuit d.c. motor, model UGPMFE - 16AAB rated at 350W, 47V. The weight of the cabin fully loaded is 460 kg.

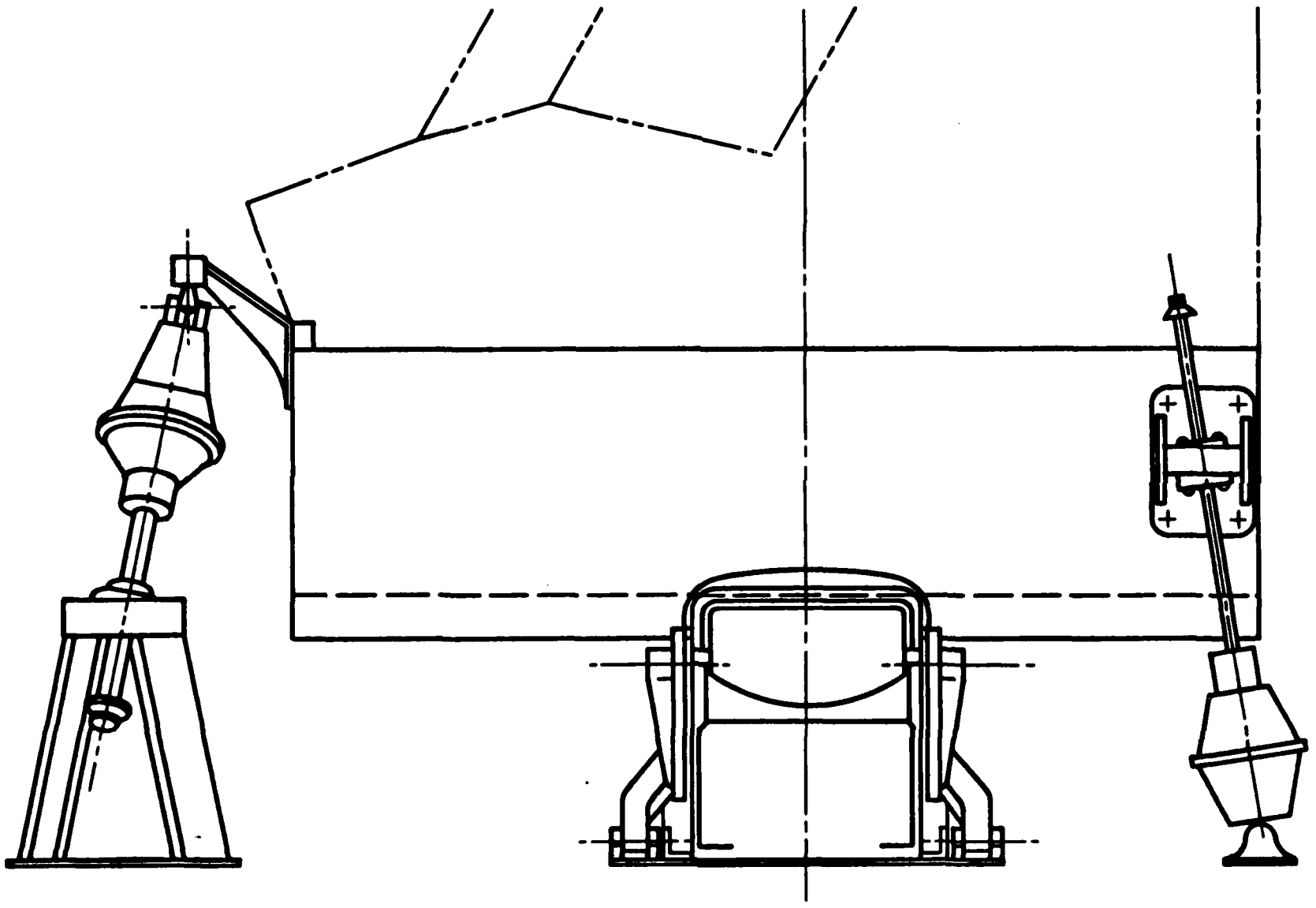

FIG. 2.1 ELEVATION VIEW OF MOTION PLATFORM SUSPENSION AND DRIVE CONFIGURATION

2.2 Motor/Load Model

If a voltage V is applied to a motor with armature resistance r_a the gross electrical torque, T, is given by -

$$T = k_T I \quad ; \quad V = E + r_a I$$

where I is the current in amps, E is the e.m.f. in volts and k_T is the motor torque constant. Noting that at speed w the e.m.f. constant k_E is equal to E/w and since electrical power available for conversion must equal gross mechanical output power (EI = Tw) the motor equation reduces to -

$$V = k_T w + \frac{r_a}{k_T} T \; . \qquad ..(2.1)$$

Now, gross torque, T, is given by -

$$T = k_D w + T_F + T_O \qquad ..(2.2)$$

where k_D is the damping torque constant, T_F is the Coulomb friction torque and T_O is the available output torque. Combining (2.1) and (2.2) the speed-torque characteristic of the motor is -

$$T_O = \left(\frac{V k_T}{r_a} - T_F \right) - w f \qquad ..(2.3)$$

where

$$1/f = \frac{r_a}{k_T^2 + k_D r_a}$$

is motor regulation (reduction in speed per unit change in load torque). Typically for motors over 300W, k_D is 2% of (k_T^2/r_a) [1] and hence f can be taken as -

$$f \simeq k_T^2/r_a .$$

Now for an inertial load J, and spring restoring load torque $k_s\theta$, where θ is the motor angle, the dynamic equation of the motor is -

$$J \frac{dw}{dt} = \frac{V k_T}{r_a} - fw - k_s\theta - T_F \; .$$

Taking Laplace transforms, the linear system transfer function is -

$$\frac{\Omega(s)}{V(s)} = \frac{k_T}{r_a} \cdot \frac{s}{Js^2 + fs + k_s} \qquad ..(2.4)$$

where s is the Laplace transform variable and $\Omega(s)$ and V(s) are the Laplace transforms of the motor velocity and the applied motor voltage respectively. A block diagram of the system is shown below (Figure 2.2).

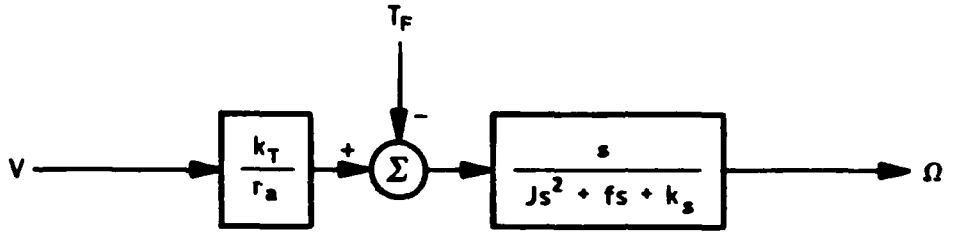

FIG. 2.2 MOTOR/LOAD MODEL

The range of load parameters, referred to motor shaft, as determined by consideration of the inertia and load torque of individual motors for motion in each degree of freedom, are -

$$0.002 \leq J \leq 0.006 \text{ kg m}^2$$

$$0.02 \leq k_s \leq 0.03 \text{ Nm/rad.}$$

For pitch and yaw motion the spring restoring torque is negligible in which case k_s can be assumed zero. The measured estimates of Coulomb friction are -

$$\text{static friction, } T_s = 0.25 \text{ Nm}$$

$$\text{running friction, } T_R = 0.2 \text{ Nm.}$$

2.3 Control System Configuration

Figure 2.3 shows the computer control configuration for each servomotor at a sampling period of Δt seconds. The control computer samples the reference input and system output both of which are available in digital form. The reference velocity input is computed by the flight simulation computer whilst the control computer calculates the motor velocity from the output of the shaft position encoder which has a resolution of 1/600 revolution of the motor shaft. It will be assumed that the encoder is linear with bandwidth sufficiently great compared to the system bandwidth such that its dynamics need not be considered in the subsequent analysis.

In operation the control computer calculates the system velocity error and computes the control which is to be applied to the system, via a zero order hold circuit, one sampling period later. This computation/control delay is represented in the model by the transfer junction $e^{-s\Delta t}$. Although the d.c. servo amplifier is represented in the configuration of Figure 2.3, it will be assumed to have a bandwidth such that its analytic representation is just a pure gain in the control law.

2.4 Performance Specification

The aim of the control system design is to derive a control algorithm that will maintain closed loop system stability and performance under a range of system parameters and load conditions. In general the specification of the performance of a motion base platform involves the characteristics of the actuators, platform dynamics, the aircraft to be simulated and the physiology of human motion sensory system. In the present case consideration is limited to the individual actuator loops and hence control system performance can be adequately specified in terms of accepted servomechanism criteria.

Specifically, for a sampling period -

$$\Delta t = 0.02 \text{ sec.}$$

and for nominal system parameter values of -

$$J = 4 \times 10^{-3} \text{ kg m}^2$$

$$k_s = 2.5 \times 10^{-3} \text{ Nm/rad}$$

the compensated open loop system is to have

(i) 8db gain margin;

(ii) 45° (minimum) phase margin; and

(iii) closed loop system bandwidth (3db) of 5 Hz.

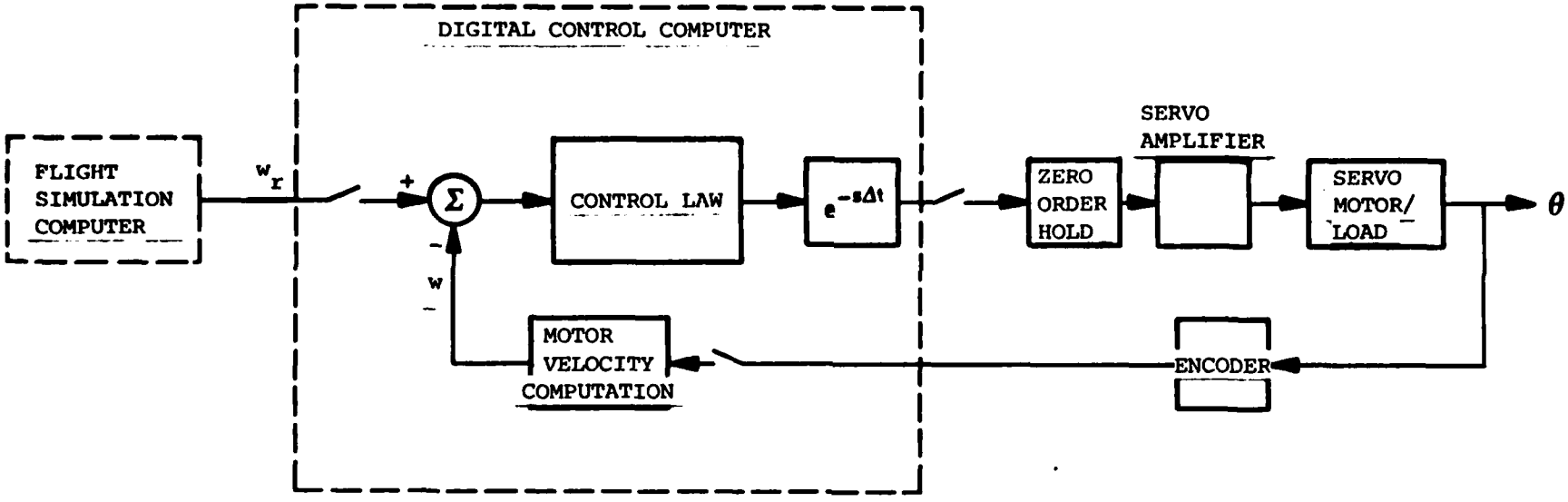

FIG. 2.3 DIGITAL CONTROL CONFIGURATION

The choice of sampling interval is primarily dictated by the computational capability of the LSI-11/02 subject to the requirement that a multiplexed four channel control system is to be realized. The gain and phase margin specifications reflect closed loop system stability with respect to system parameter variations whilst closed loop bandwidth is derived from the reference input bandwidth which is estimated to be no greater than 2 Hz. The bandwidth requirement will ensure adequate speed of response.

In addition to the above requirements a further measure of the tracking accuracy of the closed loop system can be specified as follows: let the time translated sum of squares velocity error be defined as -

$$S_w(j) \triangleq \sum_{k=0}^{\infty} \left(w(k\Delta t) - w_r(\overline{k+j}\ \Delta t) \right)^2$$

and define the "average" time delay of response as -

$$\text{average time delay} = \ell \Delta t$$

where

$$\ell = \min_j S_w(j) .$$

Then a "global" measure of distortion is given by the rms quantity -

$$R_w = \sqrt{\frac{1}{N} S_w(\ell)} \Big/ \sqrt{\frac{1}{N} \sum_{k=0}^{N^1} w_r^2 (k\Delta t)}$$

where $N\Delta t$ is the maximum of the duration of the motor response and the reference input. Defining $S_{\dot{w}}$, the time translated sum of squares acceleration error, analogous to S_w, a measure of acceleration tracking error is given by -

$$R_{\dot{w}} = \sqrt{\frac{1}{N} S_{\dot{w}}(\ell)} \Big/ \sqrt{\frac{1}{N} \sum_{k=0}^{N^1} \dot{w}_r (k\Delta t)^2}$$

and reflects the fidelity with which accelerations, and hence forces, can be imposed upon the crew in the simulator.

Since the present study is limited to actuator control rather than total platform control, bounds on rms tracking errors are given only for sample reference inputs derived below.

Specifically these bounds are -

$$R_w \leq 0.1$$

$$R_w(\ell) \leq 0.5$$

and

$$\ell\Delta t \leq 60 \text{ msec.}$$

The latter bound is set so as to allow adequate time for reference input computation and still keep the total cue generation time below 100 msec; the delay time often quoted for the onset of pilot induced oscillation. On the other hand the bounds on rms tracking errors are only estimates constrained by encoder accuracy; a more expedient and elegant approach, which is to be employed in the design of the overall control system for the motion platform, is to include the tracking error in the performance index of an optimal control formulation of the control law design.

Finally, the threshold velocity error limit at which the actuator is to pull free from static friction is taken as 0.67 rad/sec.

2.5 Sample Reference Velocity Inputs

The time profile of motion platform cues consist of two phases: the first is the "alerting" or "onset" phase during which the platform motion produces pilot sensed motion cues, whilst during the second phase or "washout" the platform is driven below subliminal rates back to the neutral position. The choise of onset time, magnitude of a motion cue and washout is a compromise between maximum velocity, acceleration and extension of platform actuators and the subliminal levels of motion perception. That is, for washout at below subliminal acceleration and velocity rates, a large onset cue requires long actuator travel.

For the present purposes of actuator controller design two reference velocity inputs have been derived based on an onset time of 0.25 sec, maximum actuator travel equal to 75 percent of maximum extension, with the subliminal acceleration and velocity levels quoted in [2] taken as being indicative of thresholds of motion sensation. The reference inputs, w_{r1} and w_{r2}, are shown in Figure 2.4 with w_{r1} corresponding to motion in the vertical axis and w_{r2} to motion in one of the rotational degrees of freedom.

3. CONTROL COMPENSATOR SYNTHESIS

3.1 Basic Considerations

As a starting point for digital controller design a proportional plus integral (PI) control law of the form -

$$V(s) = k_p \left(1 + \frac{k_i}{s} \right) (\Omega_R(s) - \Omega(s)) \qquad ..(3.1)$$

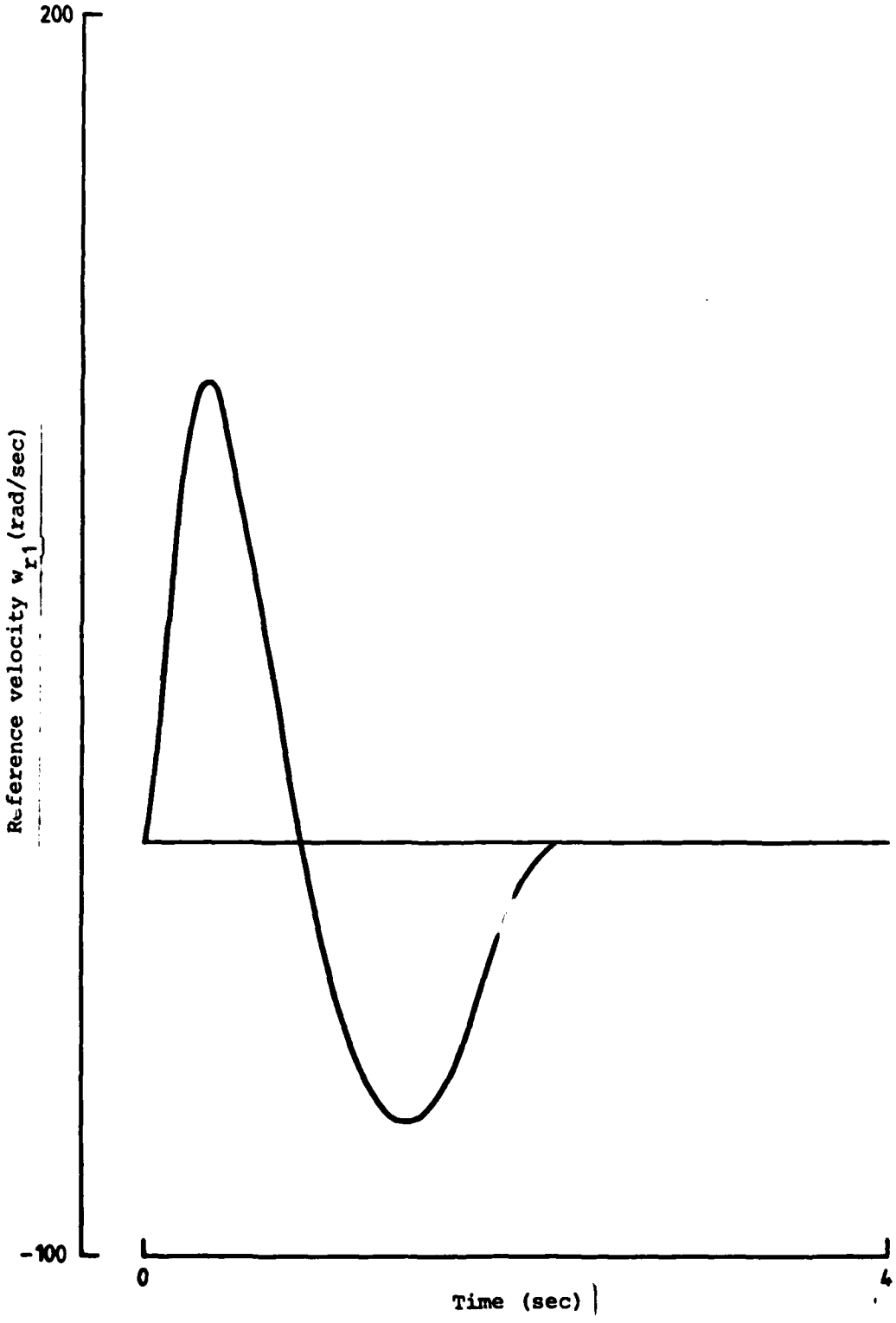

FIG. 2.4 (a) REFERENCE INPUT W_{r1}

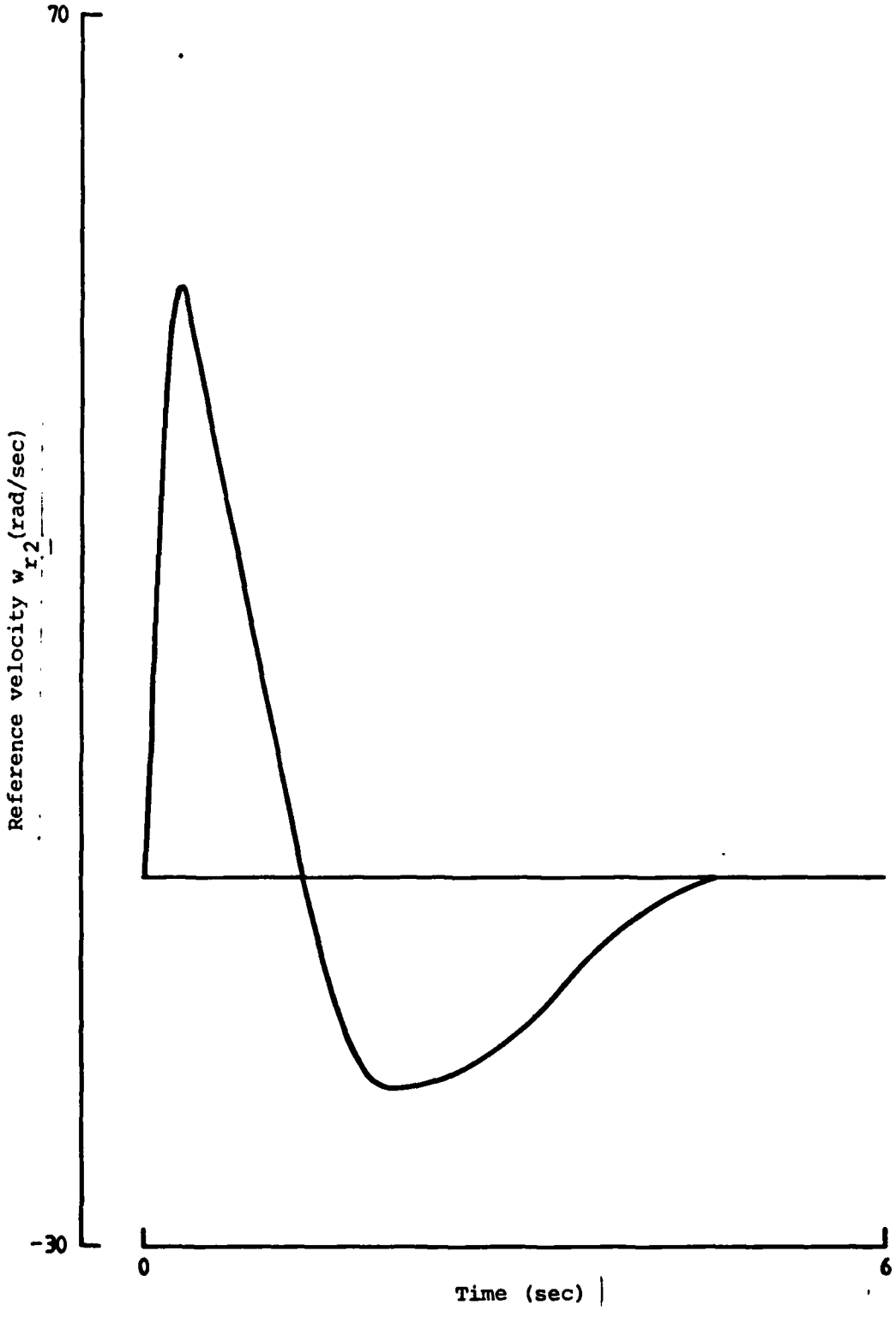

FIG. 2.4 (b) REFERENCE INPUT W_{r2}

is chosen for the continuous time representation of the motor/load system excluding the effects of sampling and friction as depicted in Figure 3.1.

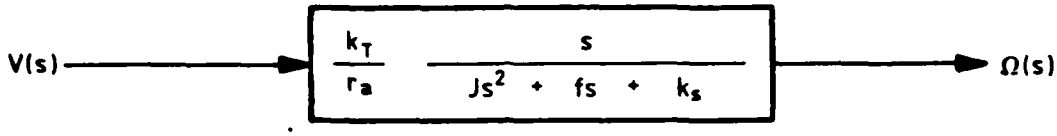

FIG. 3.1 CONTINUOUS - TIME MOTOR/LOAD MODEL

Derivative control, which would add an extra degree of freedom, is not considered since neither a sufficiently accurate estimate of acceleration is obtainable from shaft encoder measurements nor is it possible, in the present scheme, to measure armature current. The proportional and integral constants k_p and k_i are based on -

(i) pull out torque of the motor to overcome stiction; and

(ii) dominant closed loop pole placement that is relatively insensitive to spring rate, k_s, including the case $k_s = 0$.

For nominal values of system parameters -

$$J = 4 \times 10^{-3} \text{ kg m}^2$$
$$f = 1.82 \times 10^{-2} \text{ Nm/rad/sec}$$
$$k_s = 2.5 \times 10^{-2} \text{ Nm/rad}$$

the proportional gain, k_p, is selected such that the motor torque is sufficient to overcome the measured stiction torque at the velocity error threshold specified in Section 2.4, i.e.

$$k_p \frac{k_T}{r_a} (w_r - w)_{threshold} = \text{stiction torque}$$

and hence

$$k_p = 2.5 \text{ volt/volt.}$$

One the other hand root locus analysis for the two systems $k_s = 0$ and $k_s = 2.5 \times 10^{-2}$ (Figure 3.2) suggests that k_i should be chosen such that -

$$k_i > 6$$

if the closed loop characteristics of the system are to be similar for the two spring rate conditions. For the present design k_i is chosen as -

$$k_i = 15.$$

To gauge the effects on closed loop stability arising from digital realization of the PI control law, computational time delay and sampling have to be taken into consideration. For this purpose consider the model of the closed loop system depicted in Figure 3.3 where exp(-sT) and (1 - exp(-sT))/sT are three transfer functions for computer time delay and the sampler plus zero-order hold circuit [6]. Defining the open loop transfer function as -

$$T_o(s) = \frac{k_p k_T}{r_a} \exp(-sT) \frac{(1 - \exp(-sT))}{sT} \left(1 + \frac{k_i}{s}\right) \frac{s}{Js^2 + fs + k_s} \qquad ..(3.2)$$

then closed loop stability can be assessed from the Nyquist frequency of $T_o(s)$ [3]. For the values of system and control parameters the Nyquist plot of $T_o(j\omega)$ is shown in Figure 3.4. Recalling that stability of the closed loop system is assured if the graph of $T_o(j\omega)$ does not make a counter-clockwise encirclement of the -1+jo point, it can be seen from Figure 3.4 that this condition is not satisfied, and hence the closed loop system of Figure 3.3 will be unstable and additional compensation is required. The instability is due to the significant phase shift introduced by the time delay and sampler/zero-order hold circuit as shown in Figure 3.5.

3.2 Digital Control Law

Since the controller is to be realized digitally, the most convenient system description is in terms of z-transforms [3],[4]. Adopting the convention that if g(s) is the Laplace transform of g(t) then G(z) is its z-transform (with $z = e^{sT}$) the closed loop digitally controlled system is depicted in Figure 3.6 below. Here account is taken of the fact that motor speed is derived from sampled position measurements by simple differencing and reference input position is computed by rectangular integration of reference velocity input.

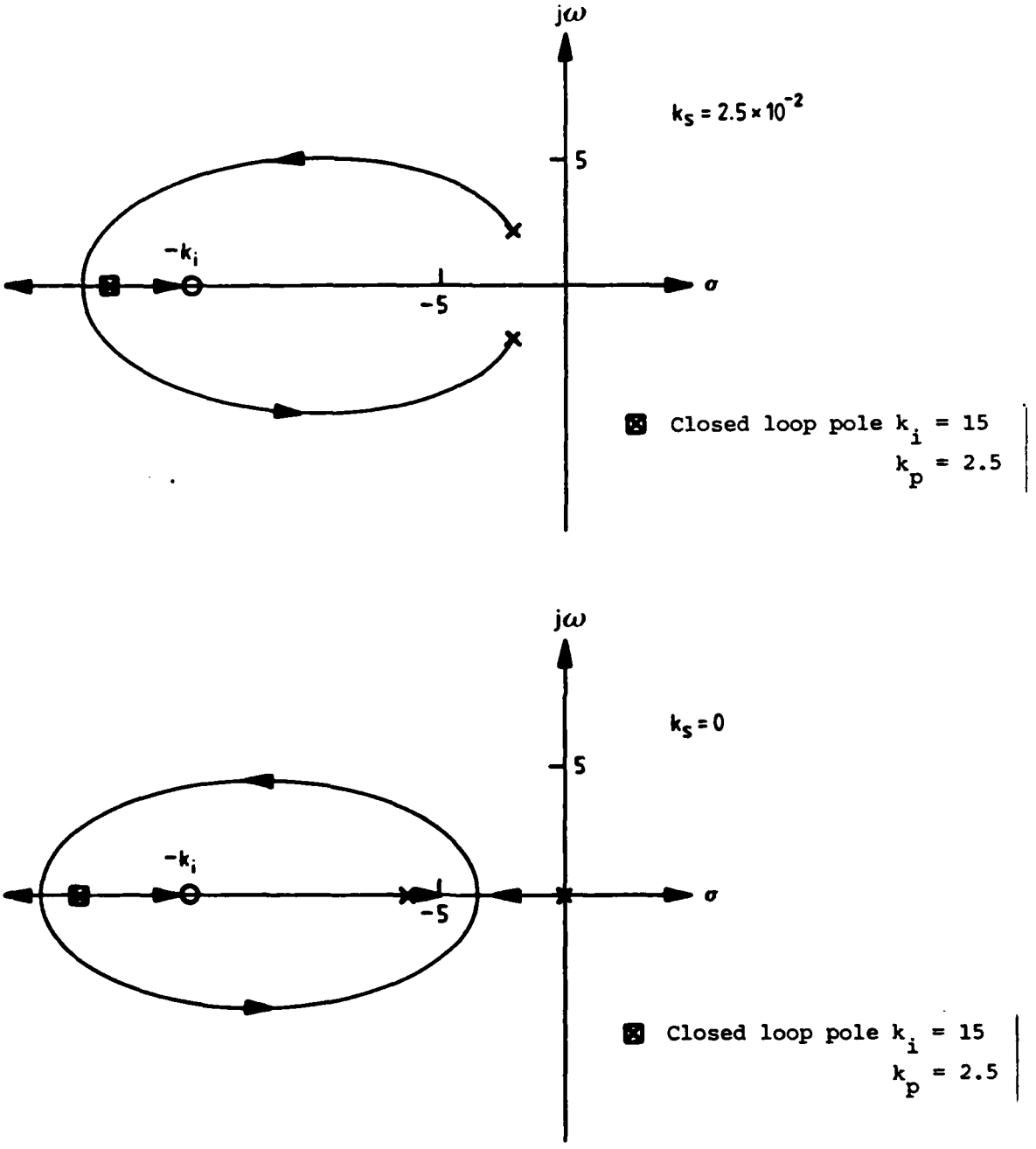

FIG. 3.2 SKETCH OF ROOT LOCUS AS A FUNCTION OF GAIN $\frac{k_p k_T}{r_a J}$

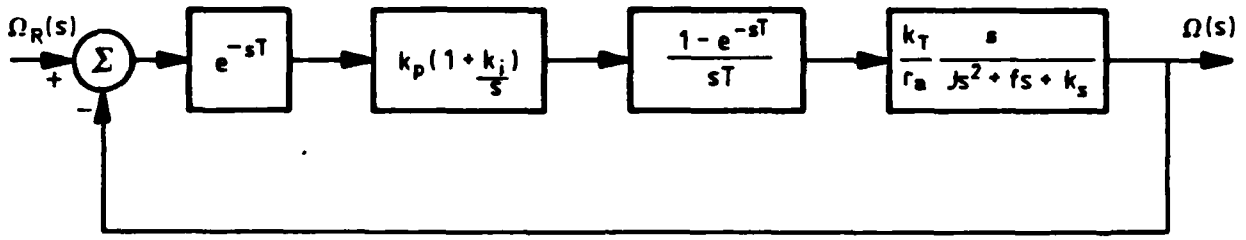

FIG. 3.3 SYSTEM MODEL INCLUDING TIME DELAY, SAMPLING AND ZERO ORDER HOLD

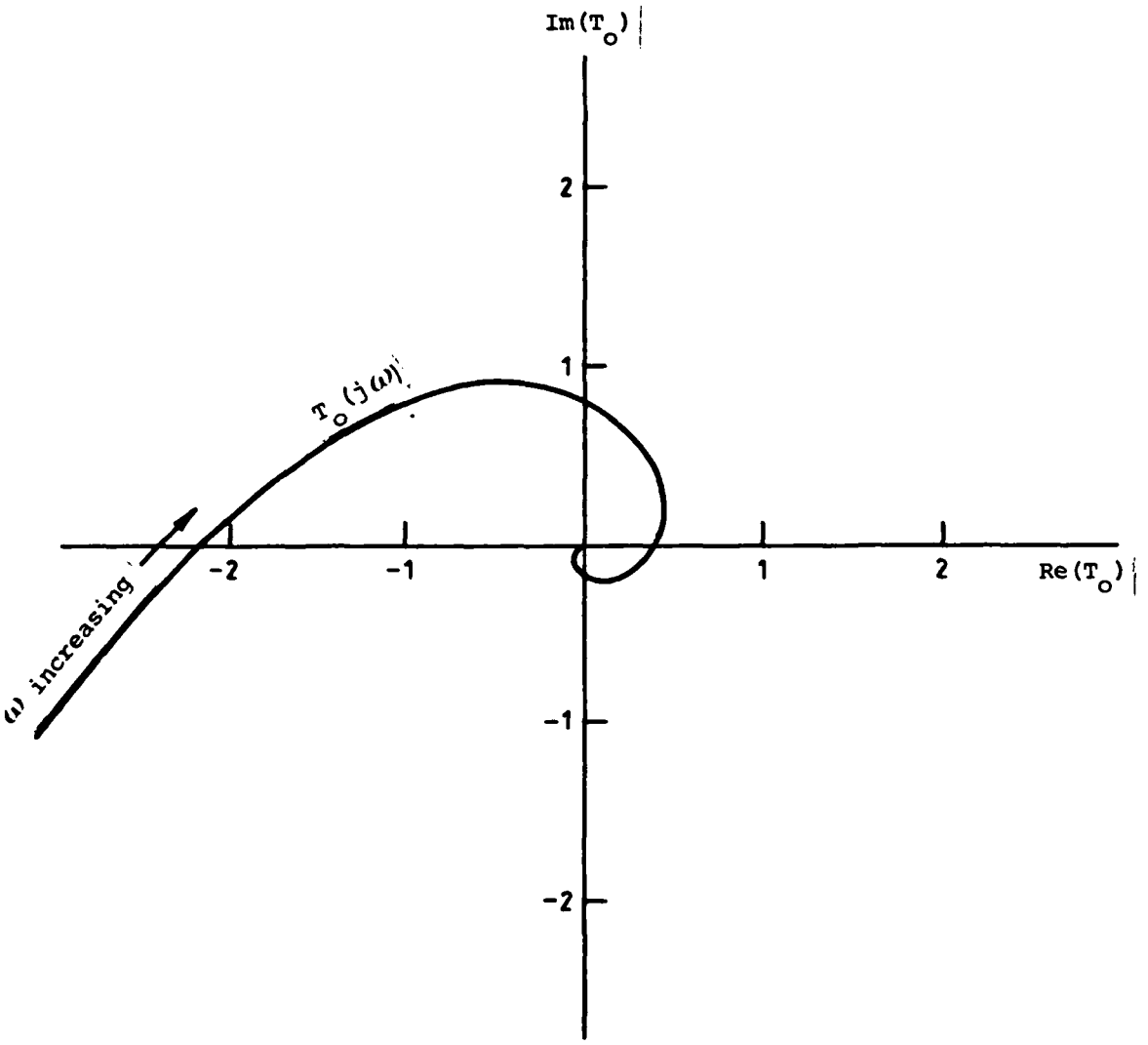

FIG. 3.4 NYQUIST PLOT OF $T_o(j\omega)$

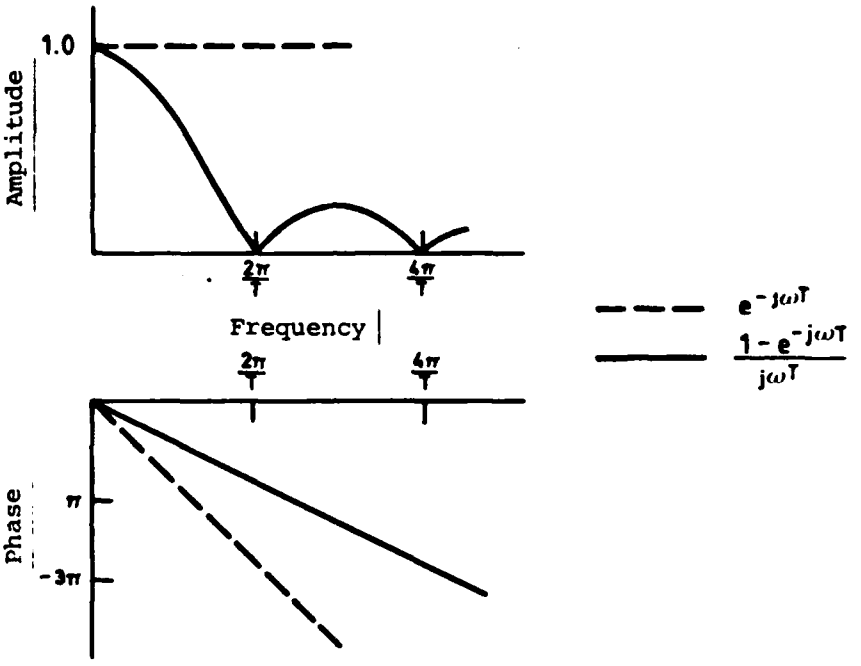

FIG. 3.5 GAIN AND PHASE OF TIME DELAY AND SAMPLER/ ZERO - ORDER HOLD TRANSFER FUNCTION

Let G(s) be the composite transfer function of the zero-order hold, motor/load and integrator with output being taken as (the physically instrumented) motor position. Then -

$$G(s) = \frac{k_T}{r_a J} \frac{s}{s^3 + 2\zeta w_n p + \omega_n^2} \cdot \frac{1}{s} \cdot \frac{1 - \exp(-sT)}{s} \qquad ..(3.3)$$

where

$$\omega_n = \sqrt{k_s/J}$$

$$\zeta = \frac{f}{2\sqrt{k_s J}} \quad .$$

Then a straight forward but messy calculation [3] gives the z-transform of G(s) as -

(i) for $k_s \neq 0$, $\zeta \leqslant 1$

$$G(z) = \frac{k_T}{r_a \omega_n^2 J}\left(1 - \frac{(z - e^{-\delta T}(\cos(\gamma T) - (\delta/\gamma)\sin(\gamma T)))\ (z-1)}{z^2 - 2ze^{-\delta T}\cos(\gamma T) + e^{-2\delta T}}\right) \qquad ..(3.4a)$$

and $\delta = \zeta w_n$

$$\gamma = w_n \sqrt{1 - \zeta^2} \ ;$$

(ii) for $k_s \neq 0$, $\zeta > 1$

$$G(z) = \frac{k_T}{r_a J \omega_n^2}\left(1 + \frac{(z-1)}{\delta - \gamma}\left(\frac{\gamma}{z - e^{-\delta T}} - \frac{\delta}{z - e^{-\gamma T}}\right)\right) \qquad ..(3.4b)$$

and $\delta = \omega_n (\zeta + \sqrt{\zeta^2 - 1})$

$$\gamma = \omega_n (\zeta - \sqrt{\zeta^2 - 1})$$

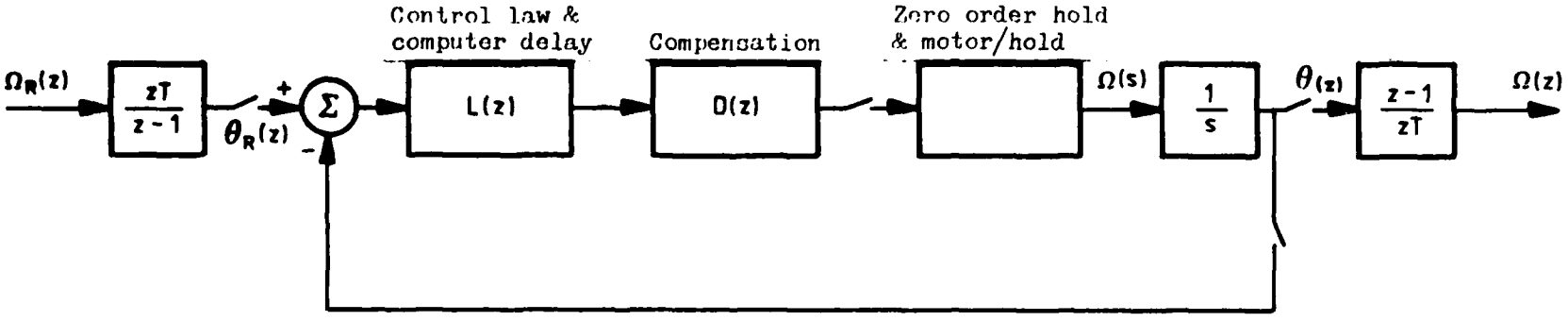

FIG. 3.6 SAMPLED - DATA MODEL OF SYSTEM

(iii) for $k_s = 0$

$$G(z) = \frac{k_T}{r_a J \delta^2} \frac{z(\delta T - 1 + \gamma) + (1 - \gamma - \delta\gamma T)}{z^2 - (1 + \gamma)z + \gamma} \quad ..(3.4c)$$

$$\delta = f/J$$

$$\gamma = e^{-\delta T} .$$

Computing motor velocity, w, by simple differencing of motor position and computing reference input position, θ_r, by rectangular integration, the z-transform of the control law, including computation delay is -

$$L(z) = \frac{k_p}{z} \left(\frac{z-1}{zT} + k_i \right) \quad ..(3.5)$$

Taking the form of compensation to be a second order section with transfer function -

$$D(z) = \left(\frac{b_1 z^2 + b_2 z + b_3}{a_1 z^2 + a_2 z + a_3} \right) \quad ..(3.6)$$

then the closed loop system transfer function is given by -

$$F_{CL}(z) = \frac{F_o(z)}{1 + F_o(z)} \quad ..(3.7)$$

with

$$F_o(z) = L(z)\, D(z)\, G(z). \quad ..(3.8)$$

The choice of compensator parameters is dictated by examination of closed loop system stability. This is accomplished by evaluating the open loop transfer function $F_o(z)$ along the unit circle $|z| = 1$. Equivalently, via the bilinear transformation -

$$z = \frac{r + 1}{r - 1} , \; r = j\omega_r$$

the stability of the closed loop system is determined by the Nyquist plot of $\hat{F}_o(j\omega_r)$,

$$\hat{F}_o(j\omega_r) \triangleq F_o\left(\frac{j\omega_r + 1}{j\omega_r - 1} \right)$$

as ω_r varies from $-\infty$ to 0 [4], where ω_r can be viewed as a "generalized frequency". Analogously to the continuous time case, counter-clockwise encirclement of the -1 + jo point by $\hat{F}_o(j\omega_r)$ implies instability of the closed loop system.

An interactive computer program with graphics capability was utilized for stability analysis and compensator design. Firstly, to counter the phase lag introduced by sampling and computation delay, lead compensation was considered with parameters -

$$a_1 = b_1 = 0,\ a_2 = 1.0,\ b_2 = 0.4,\ a_3 = b_3 = -0.33$$

for $J = 4\text{x}10^{-3}$, $k_s = 2.5\text{x}10^{-2}$. The Nyquist plot of this design is shown in Figure 3.7(a). Clearly the closed loop system is stable but the gain margin is only 1.6 db and there will be a resonance at $\omega_r \approx 2$. Moreover for small inertia ($J = 2\text{x}10^{-3}$) lead compensation alone will not stabilize the system as shown in Figure 3.7(b). Hence increasing the order of the compensator is required to give additional degrees of freedom to maintain phase lead and reduce gain at the phase crossover frequency. A design choice for D(z) of

$$a_1 = 12 \qquad a_2 = -10 \qquad a_3 = 2$$

$$b_1 = 2.2 \qquad b_2 = -2.5 \qquad b_3 = 0.72$$

gives the required improvement in gain margin and stability to low inertial load as shown in Figure 3.8. Further the stability of the closed loop system in the presence of variations in load inertia and spring constant is established by the Nyquist plots of Figure 3.9. The closed loop frequency response for the control/compensator design and $J = 4\text{x}10^{-3}$, $k_s = 2.5\text{x}10^{-2}$ is obtained by plotting magnitude and phase of

$$F_{CL}(z)\Big|_{z = e^{j2\pi fT}}$$

as in Figure 3.10, with 3db bandwidth being 7 Hz and 45° phase shift at 2 Hz.

3.3 System Stability in the Presence of Static and Sliding Friction

To complete the stability analysis of the closed loop system consideration has to be given to the presence of nonlinearities. In the present case the dominant nonlinearity in the loop is static and sliding friction (since the screw jacks are typically under load, backlash can be neglected). The method of analysis to be employed to determine closed loop stability of the resultant nonlinear system is based on describing functions (DF) or harmonic linearization.

The salient features of this approach can be described by consideration of the nonlinear continuous-time system of Figure 3.11. The method is based on the assumption that if a limit cycle occurs in

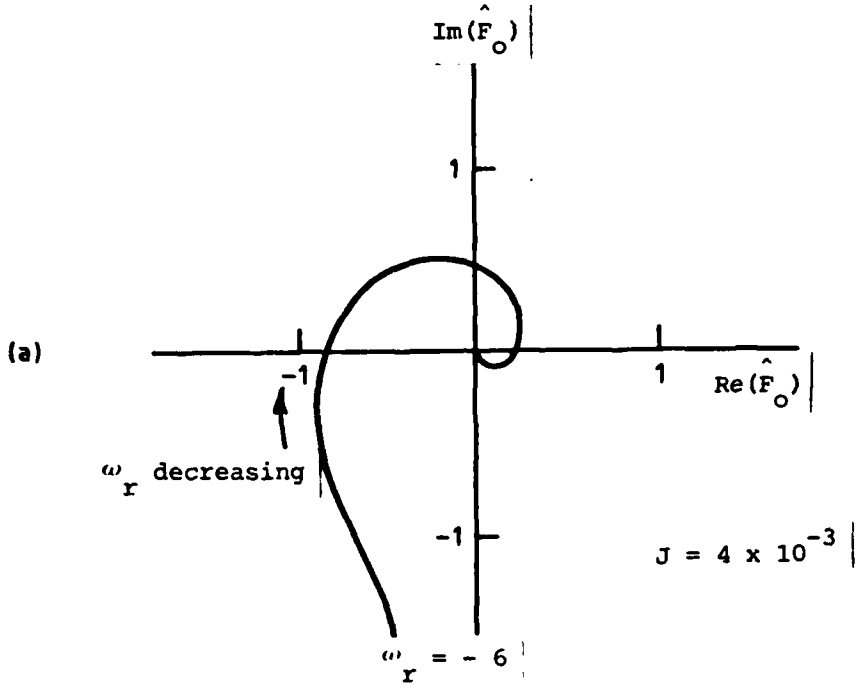

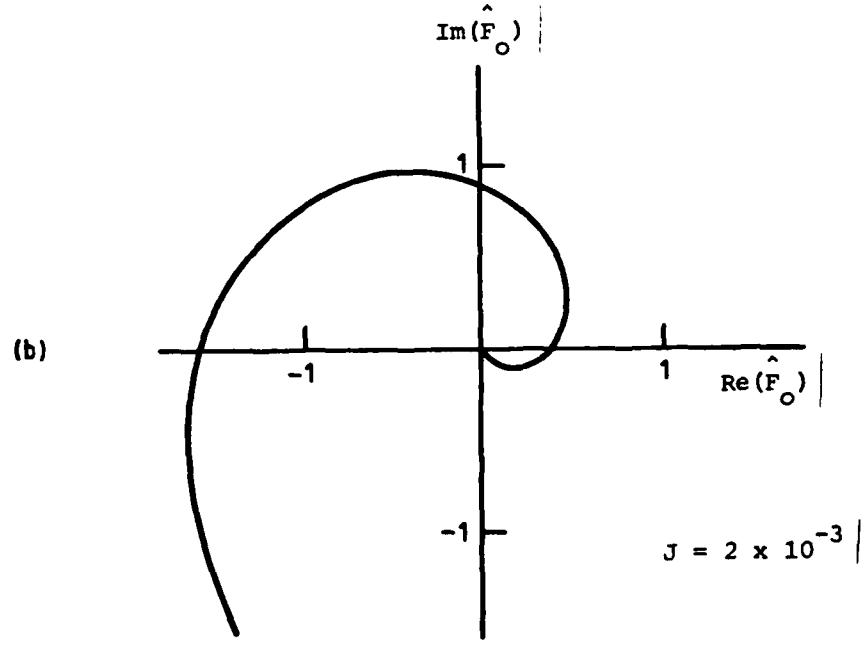

FIG. 3.7 NYQUIST PLOT - LEAD COMPENSATION

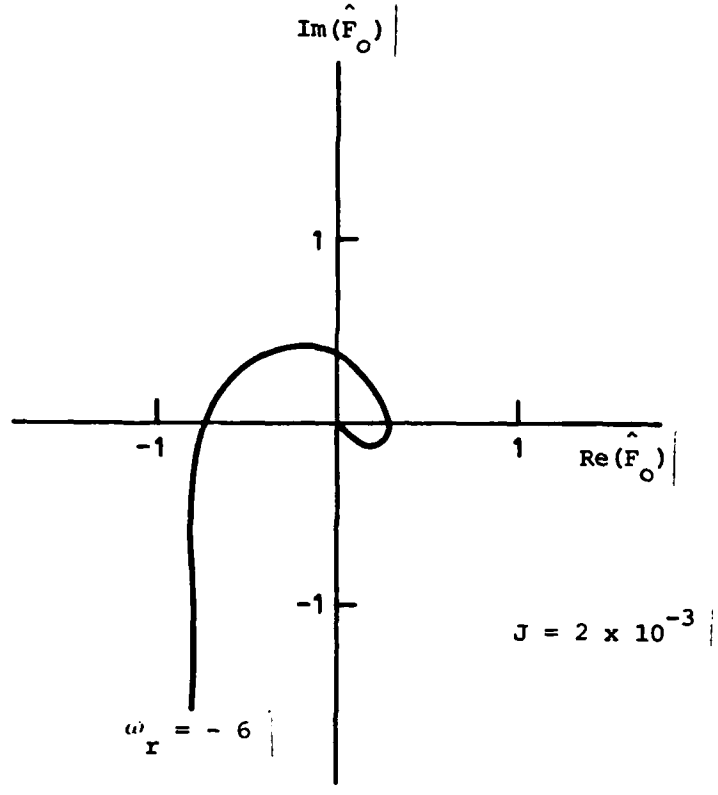

FIG. 3.8 NYQUIST PLOT FOR SYSTEM WITH SECOND ORDER COMPENSATION

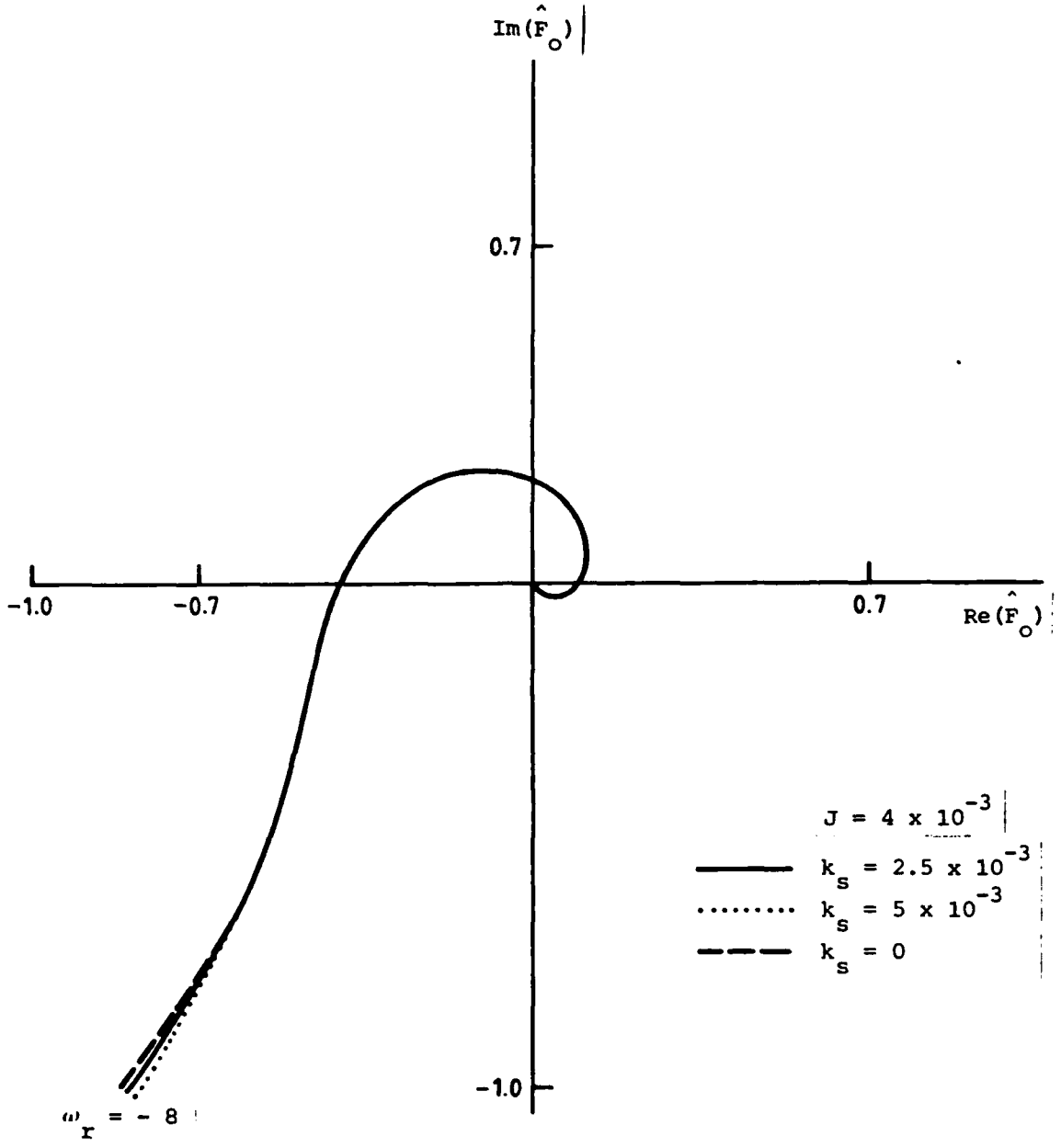

(a)

FIG. 3.9 NYQUIST PLOT - VARIATION IN SPRING CONSTANT AND INERTIA

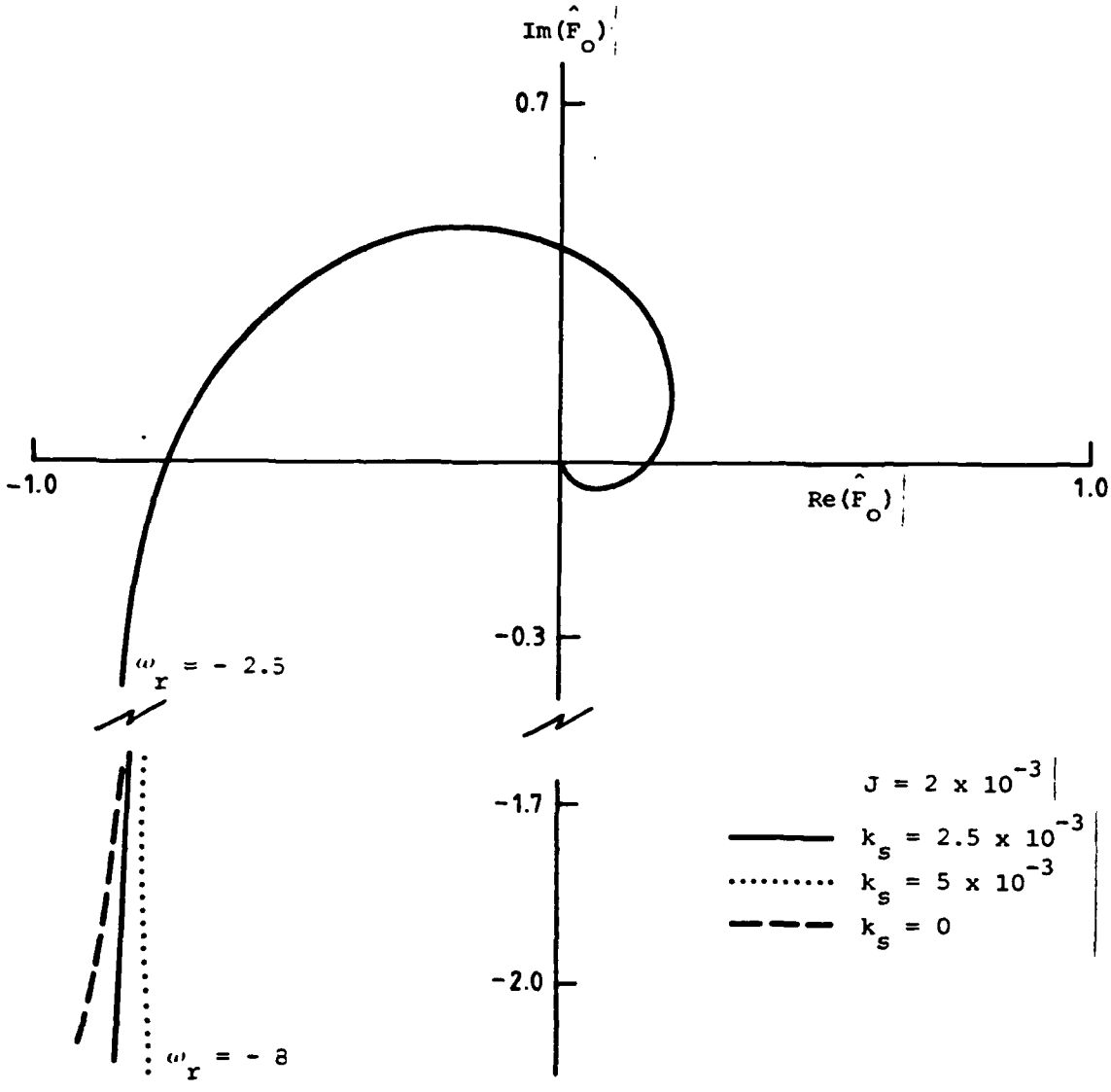
Im($\hat{F}_o$)
0.7
-1.0
Re($\hat{F}_o$)
1.0
-0.3
ω_r = - 2.5
-1.7
-2.0
ω_r = - 8
J = 2 x 10^{-3}
k_s = 2.5 x 10^{-3}
k_s = 5 x 10^{-3}
k_s = 0

(b)

FIG. 3.9 (CONT.)

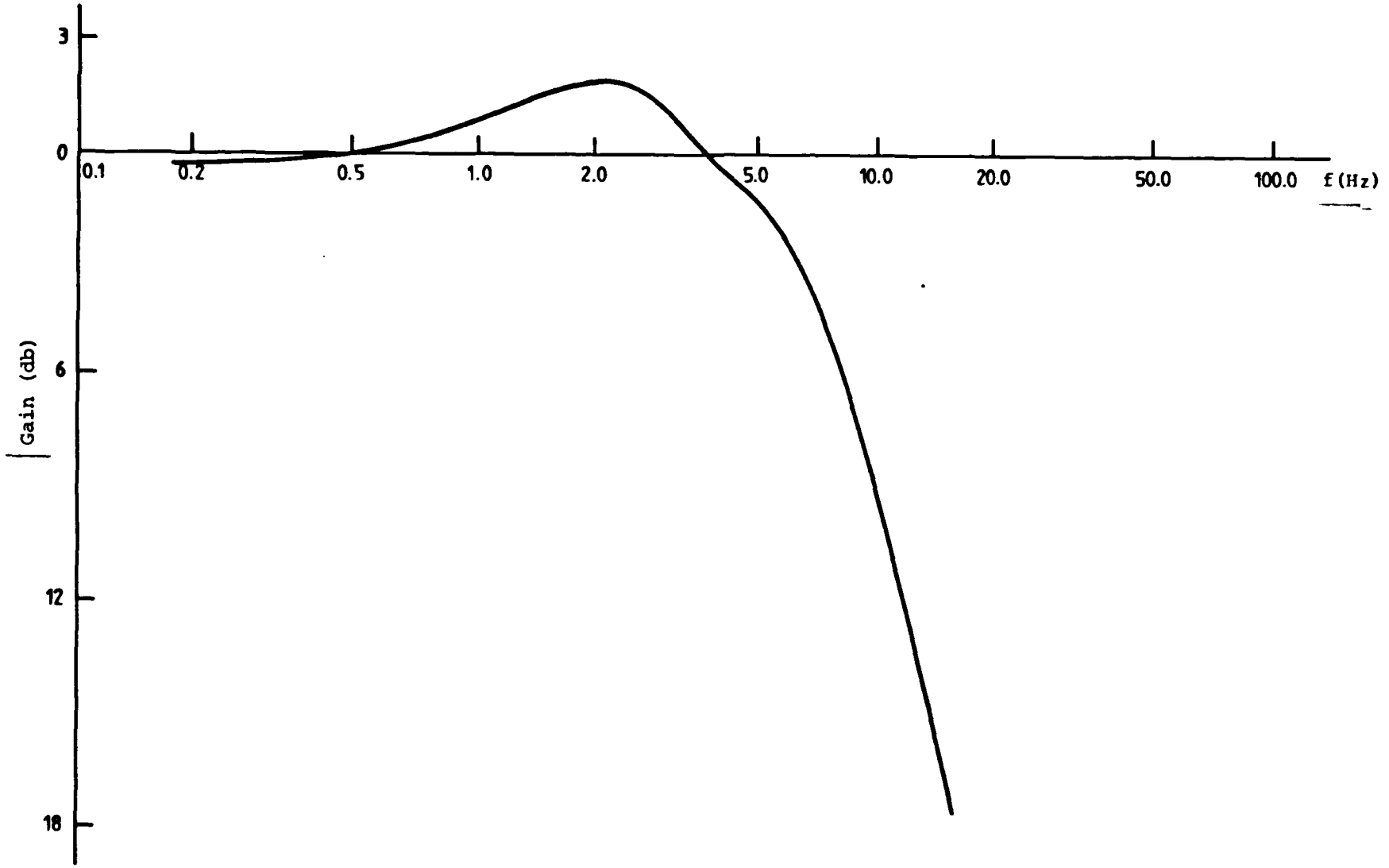

FIG. 3.10(a) CLOSED LOOP FREQUENCY RESPONSE - GAIN

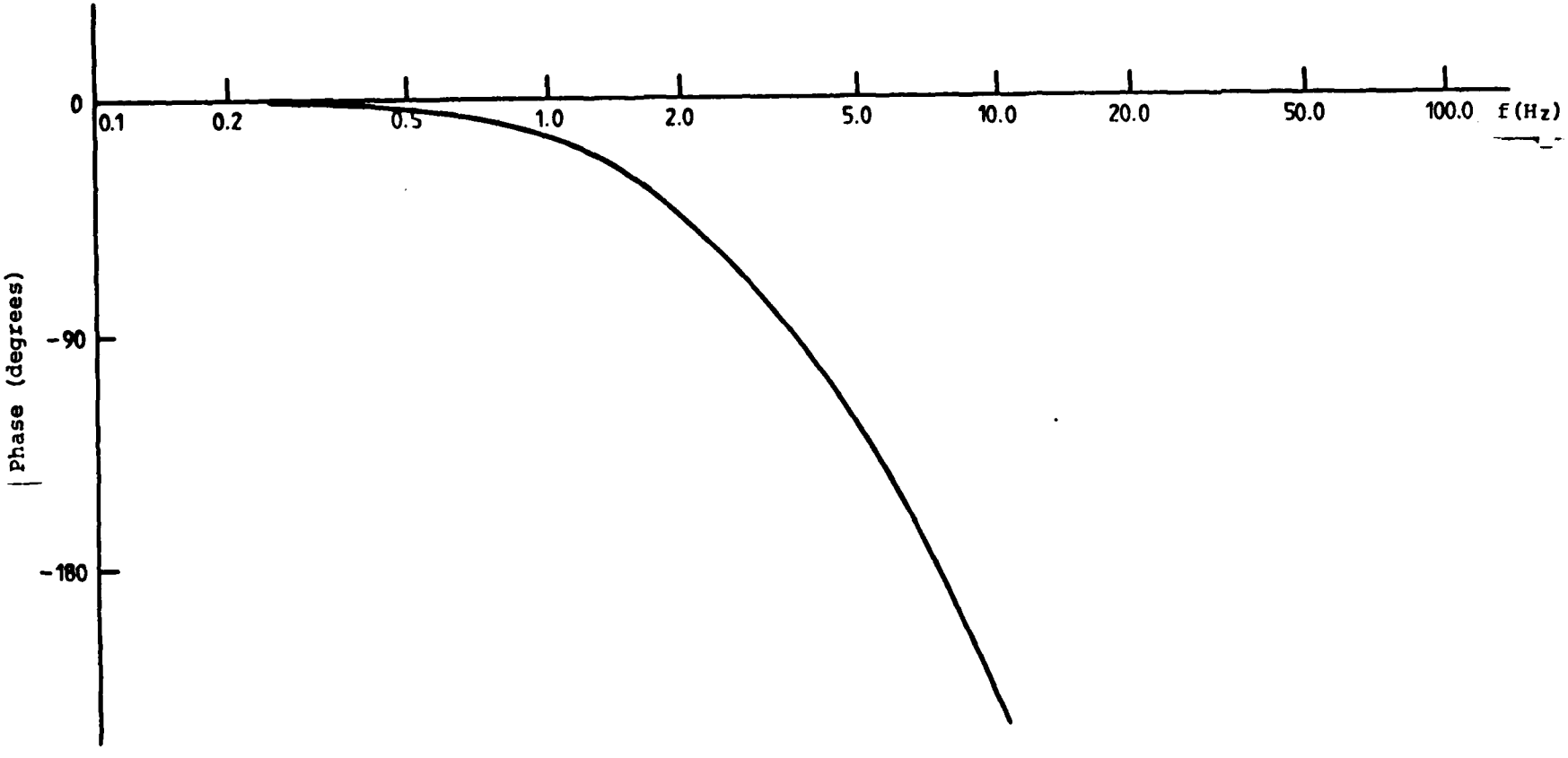

FIG. 3.10(b) CLOSED LOOP FREQUENCY RESPONSE - PHASE

the closed loop system, then as most control systems have low pass frequency characteristics, the input to the nonlinearity will be approximately sinusoidal[5]. The DF N(x) is the ratio between the input (x) and output amplitude (xN(x)) of the sinusoidally excited nonlinearity. If the nonlinearity is double valued then the DF is complex. Stability of the closed loop system is then evaluated by plotting $G_1(jw)G_2(jw)$ and $1/N(x)$ on a Nyquist diagram and applying the Nyquist criterion with respect to the locus $-1/N(x)$ instead of the point $-1+jo$. That is,[6] if -

(i) the $G_1(j\omega)G_2(j\omega)$ curve encloses the $-1/N(x)$ locus the closed loop system is unstable;

(ii) the $G_1(j\omega)G_2(j\omega)$ curve does not enclose the $-1/N(x)$ locus then the closed loop system is stable; and

(iii) the $G_1(j\omega)G_2(j\omega)$ curve intersects $-1/N(x)$ locus then a limit cycle, with amplitude and frequency determined by the point of intersection, may arise. The stability of the limit cycle is ascertained by variational techniques [5].

In the case of digital nonlinear systems describing function analysis can be carried out in one of two ways: firstly by application of the discrete describing function method developed in [4, Chp. 12], or secondly by approximating the digital elements of the control loop by frequency response equivalents and applying conventional describing function stability criteria. The first approach is specific to systems with input nonlinearities (such as relays) and requires the examination of possible limit cycles at each integral subharmonic of the sampling frequency. On the other hand the alternative approach is only valid if the digital elements of the loop are separated from the nonlinearity by continuous-time elements having low pass characteristics. In the present case, noting that the nonlinearity in question is not at the motor input and that a zero order hold is a low pass element, the second of the two approaches is adopted.

Consider the approximate model of the closed loop system depicted in Figure 3.12 where -

$$\tilde{D}(jw) = L(z)\, D(z) \Big|_{z = e^{j\omega T}}$$

is the frequency response of the digital controller including the computational delay.

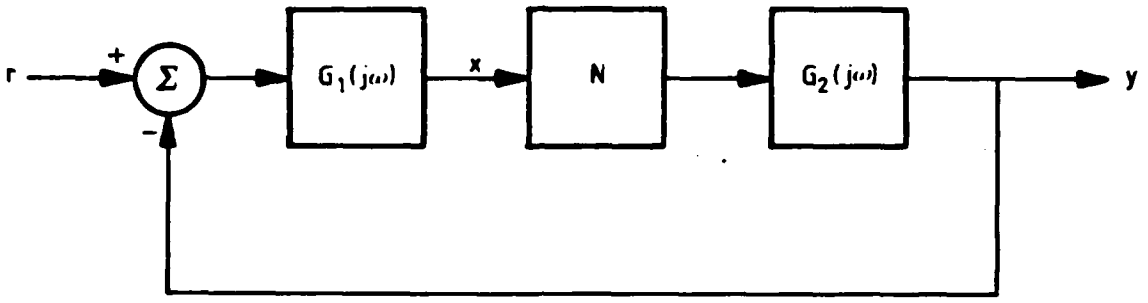

FIG. 3.11 BASIC NON-LINEAR FEEDBACK SYSTEM

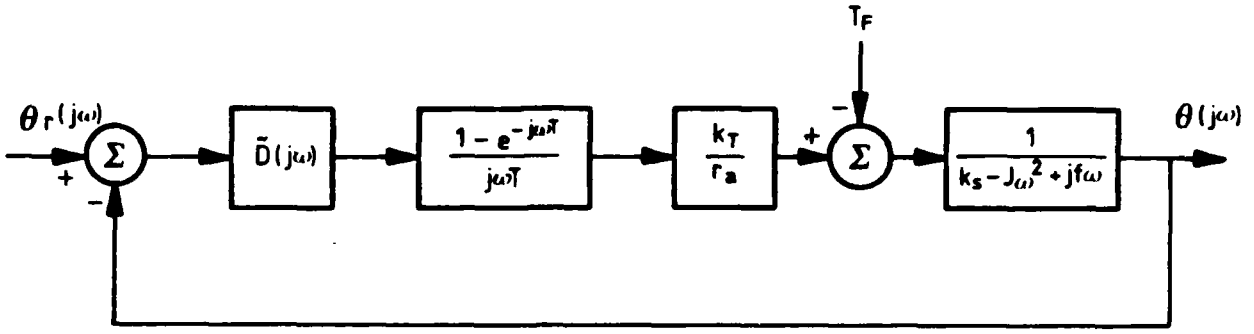

FIG. 3.12 FREQUENCY RESPONSE CHARACTERISATION OF CLOSED LOOP SYSTEM

Assuming the Coulomb friction characteristic of Figure 3.13, the describing function for friction acting on a purely inertial load has been derived in [8] and is plotted as $1/N(\lambda)$ in Figure 3.14. Here the describing function parameter is -

$$\lambda = T_R/T_a$$

with the applied torque being $T_a \sin\omega t$ and the loci terminate at $\lambda = T_R/T_s$ since $\lambda > T_R/T_s$ implies $T_a < T_s$. Rearranging the block diagram of Figure 3.12 such that friction acts on an inertial load leads to the system representation of Figure 3.15(a) and further rearrangement results in the system of Figure 3.15(b), where

$$\tilde{G}(j\omega) = \tilde{D}(j\omega) \frac{(1 - e^{-j\omega T})}{j\omega T} + \frac{k_T}{r}(k_s + jf\omega).$$

Application of the Nyquist stability criterion to the plot of $1/N(\lambda)$ and $\bar{b}(j\omega) = -k_T/r_a \tilde{G}(j\omega)/J\omega^2$ on the complex plane (Figure 3.16) readily verifies that the closed loop system will be stable for the expected range of system and Coulomb friction parameters.

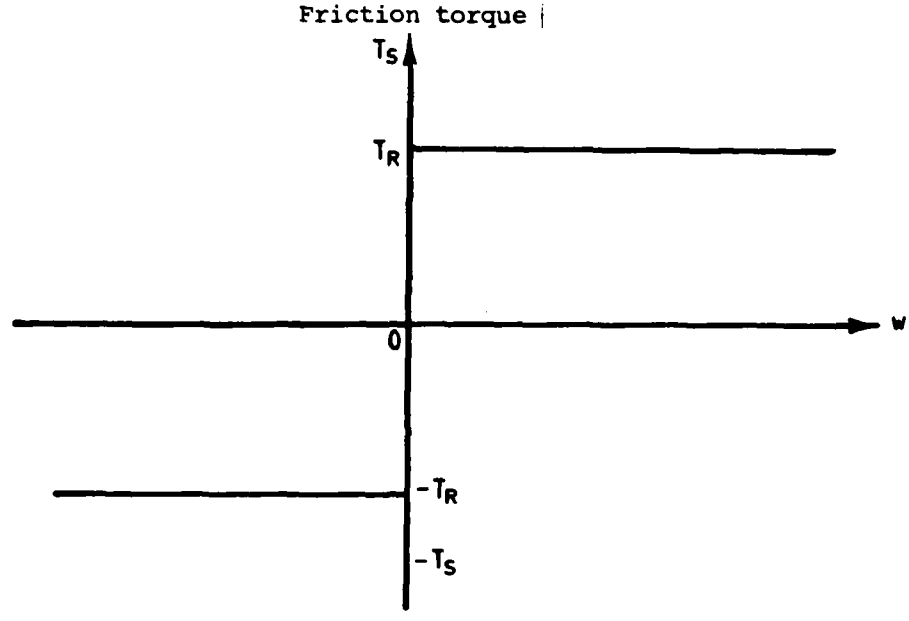

FIG. 3.13 FRICTION CHARACTERISTIC

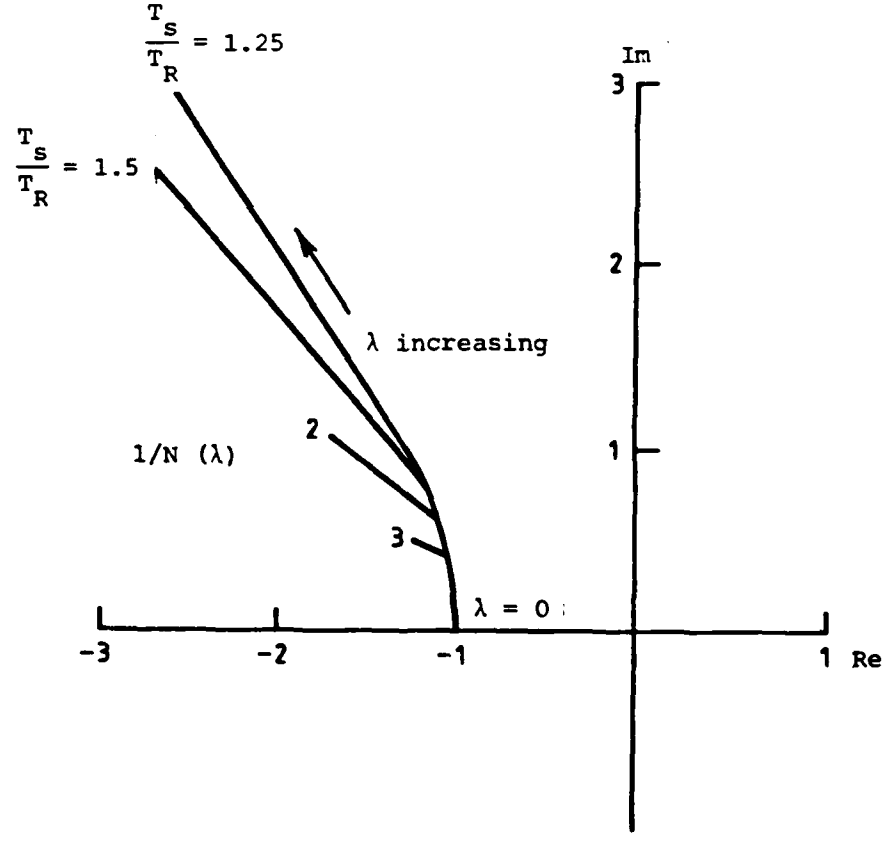

FIG. 3.14 FRICTION DESCRIBING FUNCTION

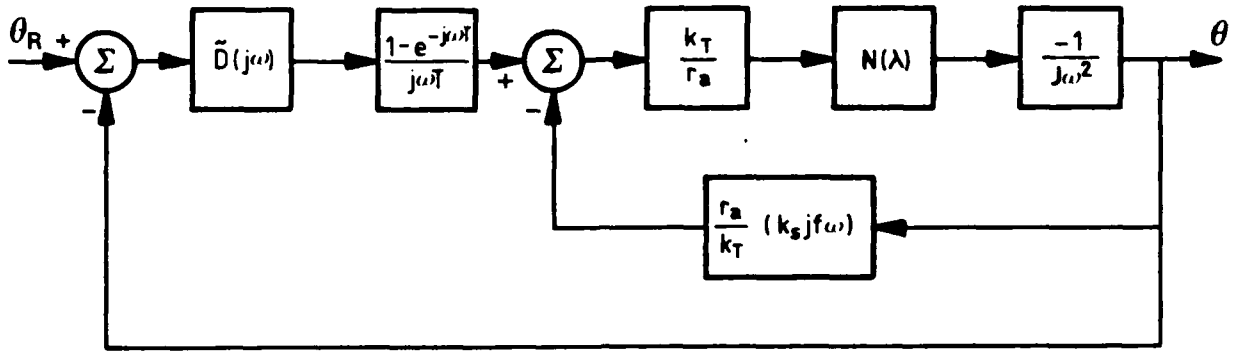

(a)

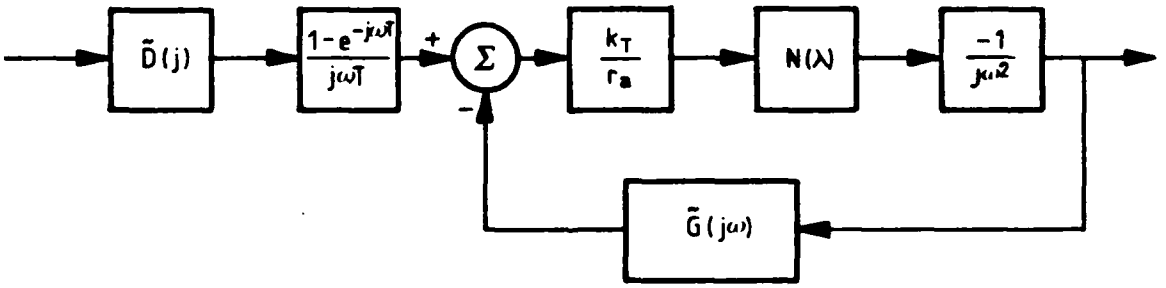

(b)

FIG. 3.15 SYSTEM TRANSFORMATION FOR DESCRIBING FUNCTION ANALYSIS

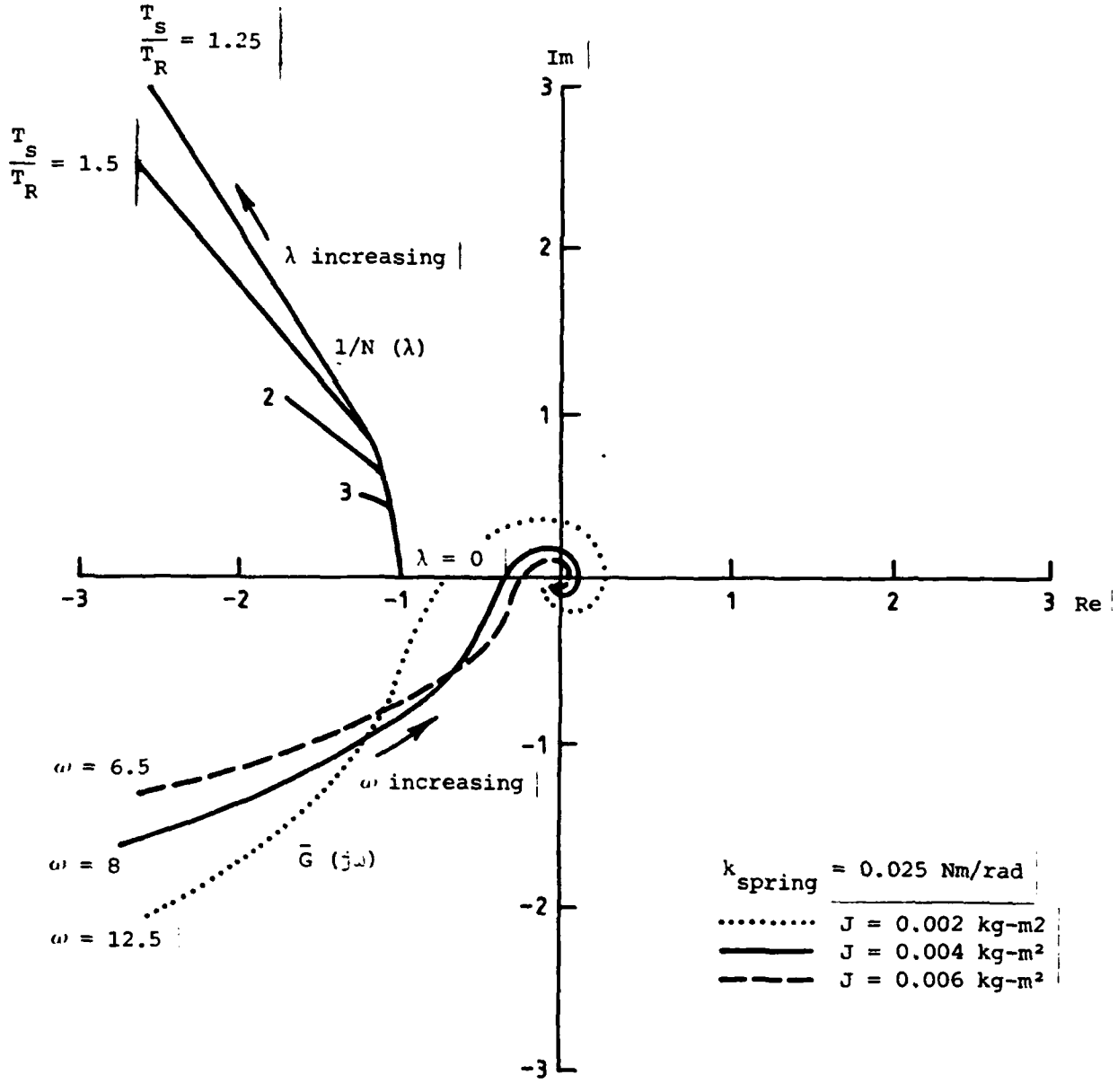

FIG. 3.16(a) DESCRIBING FUNCTION AND FREQUENCY LOCI

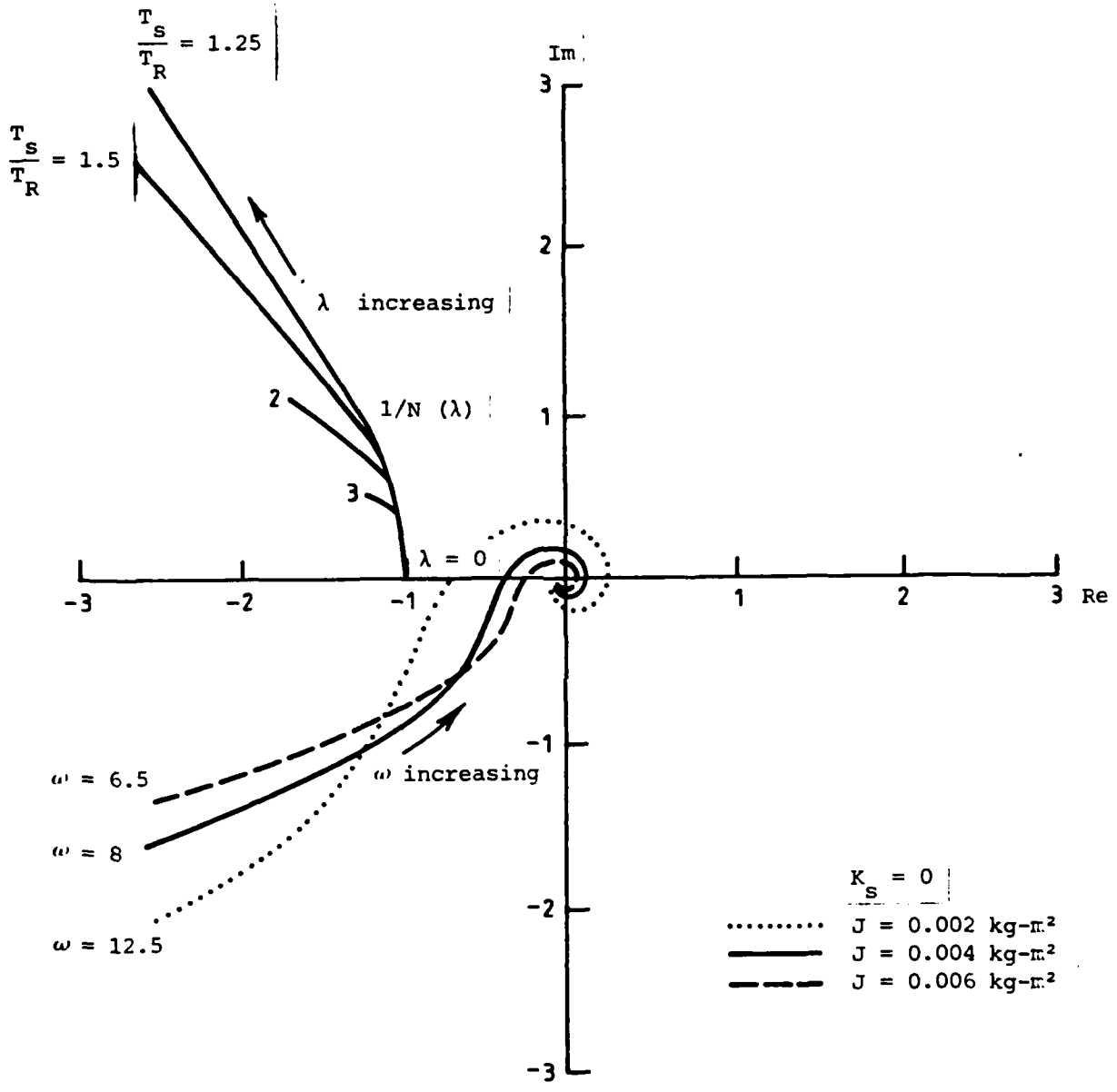
$\frac{T_s}{T_R}$ = 1.25
$\frac{T_s}{T_R}$ = 1.5
λ increasing
1/N (λ)
2
3
λ = 0
Im
Re
3
2
1
-1
-2
-3
-3
-2
-1
1
2
3
ω = 6.5
ω = 8
ω = 12.5
ω increasing
K_s = 0
J = 0.002 kg-m²
J = 0.004 kg-m²
J = 0.006 kg-m²

FIG. 3.16(b)

4. SIMULATION OF CLOSED LOOP SYSTEM

The efficacy of the digital controller design in meeting the required closed loop system performance criteria is confirmed by digital simulation. The motor model, Coulomb friction and position encoder characteristics are represented as a set of first order differential equations with algebraic constraints, and integrated using a 4th order Runge-Kutta integration routine with a step size of $0.01\Delta t$ on a DECsystem-10 computer. Included in this representation is the time delay between measurement of system states and reference input, and application of the control input. The digital compensator is simulated in recursive form, operating at a simulated sampling period of Δt seconds with motor position measurements quantized to 600 counts per revolution to emulate the position encoder. In this way the motor appears as a continuous system to the digital controller with system nonlinearities being faithfully represented.

Simulations were conducted over a range system parameters for the class of reference inputs specified in Section 2.5. The results of these are depicted in Figure A1 and the computed performance measures are tabulated in Table A1 of the Appendix. It can be readily seen that for a wide range of system parameters the closed loop system exhibits good velocity tracking and the performance measures are within the required bounds. However, for large inertia (and hence reduced motor damping), the larger initial overshoot is responsible for the performance measures being outside the prescribed bounds. This is not a critical deficiency since the initial "attack" of the response represents the cue and it is precisely here, rather than during the subsequent washout, that overshoot can be tolerated. On the other hand the increase in R_w for the low amplitude input ($0.25\ w_{r1}$) and inertia of 2×10^{-3} kg m^{-2} is due to the friction effects at the first velocity null point. Moreover, as regards friction, two observations can be made: firstly for large amplitude reference inputs (such as w_{r1}) the velocity lag error arising from the time delay between input and response at w=0 is sufficient to overcome static friction. Clearly from Figure A1(c) this is not the case for low amplitude reference inputs where the motor velocity remains zero until the magnitude of the velocity error is sufficient to overcome stiction. Secondly, the presence of friction has an ameliorating effect in that it quenches limit cycles that would normally arise from encoder rounding errors. These oscillations are evident when the system is simulated without friction (Figure A2(a)) and are reduced in amplitude when the encoder wordlength is increased from 10 to 12 bits (Figure A2(b)).

5. NONLINEAR COMPENSATION

The results of simulation indicate that the effect of friction are significant for low amplitude reference inputs, where the velocity error at zero motor velocity is insufficient to counter static friction. To overcome this, two approaches are possible: firstly one can inject high frequency dither at the motor input which has the effect of "smoothing" the nonlinearity [10] or secondly, apply additional nonlinear compensation such that the effective loop gain of the system increases in the region of zero motor velocity for low amplitude velocity error. In the present

case direct generation of dither signal by the digital control computer is not possible due to the relatively low sampling rate, and hence the alternative amplitude dependent gain approach is adopted for investigation. The development below should be taken as exploratory rather than definitive, the aim being to demonstrate the flexibility afforded by computer control for nonlinear compensation.

The difficulty of detecting the null velocity point of the response, given the sampling period and the computation delay, dictates that the nonlinear control effort becomes significant within some region of zero motor velocity, for low velocity errors and non-zero reference inputs. One smooth nonlinear function satisfying these criteria is

$$U_{NL}(k\Delta t) = C\, e_w(k\Delta t)\, \exp\left(-\alpha\, e_w(k\Delta t)^2 - \beta\, W(k\Delta t)^2\right),$$

$$e_w \triangleq w_r - w$$

where the parameter α specifies the level of velocity error beyond which linear control is sufficient to overcome static friction, β specifies the region about zero motor velocity where U_{NL} is to contribute to the control effort and C is the gain. The output, u, of the digital controller can now be taken as

$$u(k\Delta t) = u_L(k\Delta t) + u_{NL}(k\Delta t)$$

where u_L is the output of the linear controller.

The choice of parameters α, β and C are determined from the simulated response of the closed loop system to the velocity input $0.25\, w_{r1}$. For this response the velocity error at zero motor velocity is

$$e_w \Big|_{w=0} = 1.5 \text{ rad/sec.}$$

Assuming that at w=0 the additional torque produced by the nonlinear control term is approximately equal to the static friction results in

$$C(1.5)\exp(-\gamma\, 1.5^2)\ \frac{k_T}{r_a} = 0.28 \text{ Nm } (\simeq \text{ stiction}).$$

Choosing

$$\exp(\gamma(1.5)^2) = 0.8$$

gives

$$\gamma = 0.1 \quad \text{and} \quad C = 1.56.$$

Further the region about w=0 where the nonlinear control is to be active can be taken as $|w| \leq 0.5$ rad/sec with

$$1 \geq \exp(-\beta w^2) \geq 0.85 \quad ; \quad |w| \leq 0.5$$

and this leads to -

$$\beta = 0.65.$$

Results of simulation for these parameter values are shown in Figure A3, where it can be noted that the duration of zero motor velocity in the interval about t=1.8 sec has been considerably reduced compared to response of Figure A1(c). This improvement in performance is reflected in values of R_w and $R_{\dot{w}}$ as recorded in Table A2.

Little analytical machinery exists for the stability of discrete-continuous systems with multiple nonlinearities. The discrete extensions of Popov's Criterion as developed in [11] and [12] are not applicable to the present case as they are limited to one nonlinearity in the loop, whilst discrete Liaponov methods ([3]) cannot accommodate Coulomb friction. Nevertheless it can be agreed that the closed loop system will be bounded-input bounded-output stable since for large velocity errors and/or large motor velocity the nonlinear control is insignificant and bounded response will be assured by the linear analysis of Section 3.3.

6. CONCLUDING REMARKS

Frequency domain techniques together with approximate describing function analysis have been shown to offer a mathematically tractable method for the analysis and synthesis of digital control laws for a velocity tracking actuator in the presence of load variations and system nonlinearities. A significant feature of the control law is the inclusion of a nonlinear gain term to attenuate the deleterious effects of stiction for low amplitude inputs without adversely affecting the satisfactory large amplitude response.

The principal question outstanding relates to the stability analysis of closed loop nonlinear discrete time systems. The method presented here, based on continuous time describing functions, becomes cumbersome and of limited applicability to systems with multiple nonlinearities. This is of particular importance in electromechanical systems where in addition to common nonlinear effects such as backlash and saturation, consideration may have to be given to measurement and control quantization effects as well as finite computer precision. Computationally feasible stability techniques based on discrete (z-transform) system models with multiple static nonlinearities need to be developed. One approach warranting investigation is the method of Gossel [13] based on generalized superposition principles for nonlinear systems. This could offer both input/output formulation for system analysis and a mechanism for synthesizing polynomial type nonlinear control laws to achieve magnitude dependent system performance.

REFERENCES

[1] D. ROTHWELL — "Characteristics of the printed-circuit servo-motor", Control, March 1966, pp 136-139.

[2] G.J. KRON — "Advanced simulation in undergraduate pilot training: motion system development", Air Force Human Resources Laboratory. Technical Report AFHRL-TR-75-59, Vol. II, 1975.

[3] Y. TAKAHASHI et alia, — Control and Dynamic Systems, Addison-Wesley Publ. Co., Reading, Mass., 1970.

[4] B.J. KUO — Analysis and Synthesis of Sampled-Data Control Systems, Prentice-Hall, N.J., 1963.

[5] D.P. ATHERTON — "Analysis and design of nonlinear feedback systems", Proc. IEE, Vol. 128, Part D, No. 5, 1981, pp 173-180.

[6] G.J. THALER and R.G. BROWN — Analysis and Design of Feedback Control Systems, McGraw-Hill, N.Y., 1960.

[7] O.I. ELGERD — "Control Systems Theory", McGraw-Hill, N.Y. 1967.

[8] J. TOU and P.M. SCHULTHEISS — "Static and sliding friction in feedback systems", J. App. Physics, Vol. 24, No. 9, Sept. 1953, pp 1210-1217.

[9] G. FRANKLIN and J.D. POWELL — "Digital Control of Dynamic Systems", Addison-Wesley, Mass., 1980.

[10] G. ZAMES and N.A. SHNEYDOR — "Dither in nonlinear systems", IEEE Trans. Automatic Control, Vol. AC-21, Oct. 1976, pp 660-667.

[11] E.I. JURY and B.W. LEE — "On the absolute stability of nonlinear sampled data systems", IEEE Trans. Automatic Control, Vol. AC-9, Oct. 1964, pp 551-554.

[12] R.P. IWENS and A.R. BERGEN — "Frequency criteria for bounded-input bounded-output stability of nonlinear sample-data systems", IEEE Trans. Automatic Control, Vol. AC-12, Feb. 1967, pp 46-53.

REFERENCES (CONT.)

[13] M. GOSSEL "Nonlinear Time-Discrete Systems", Lecture Notes in Control and Information Sciences, Springer-Verlag, Berlin, 1982.

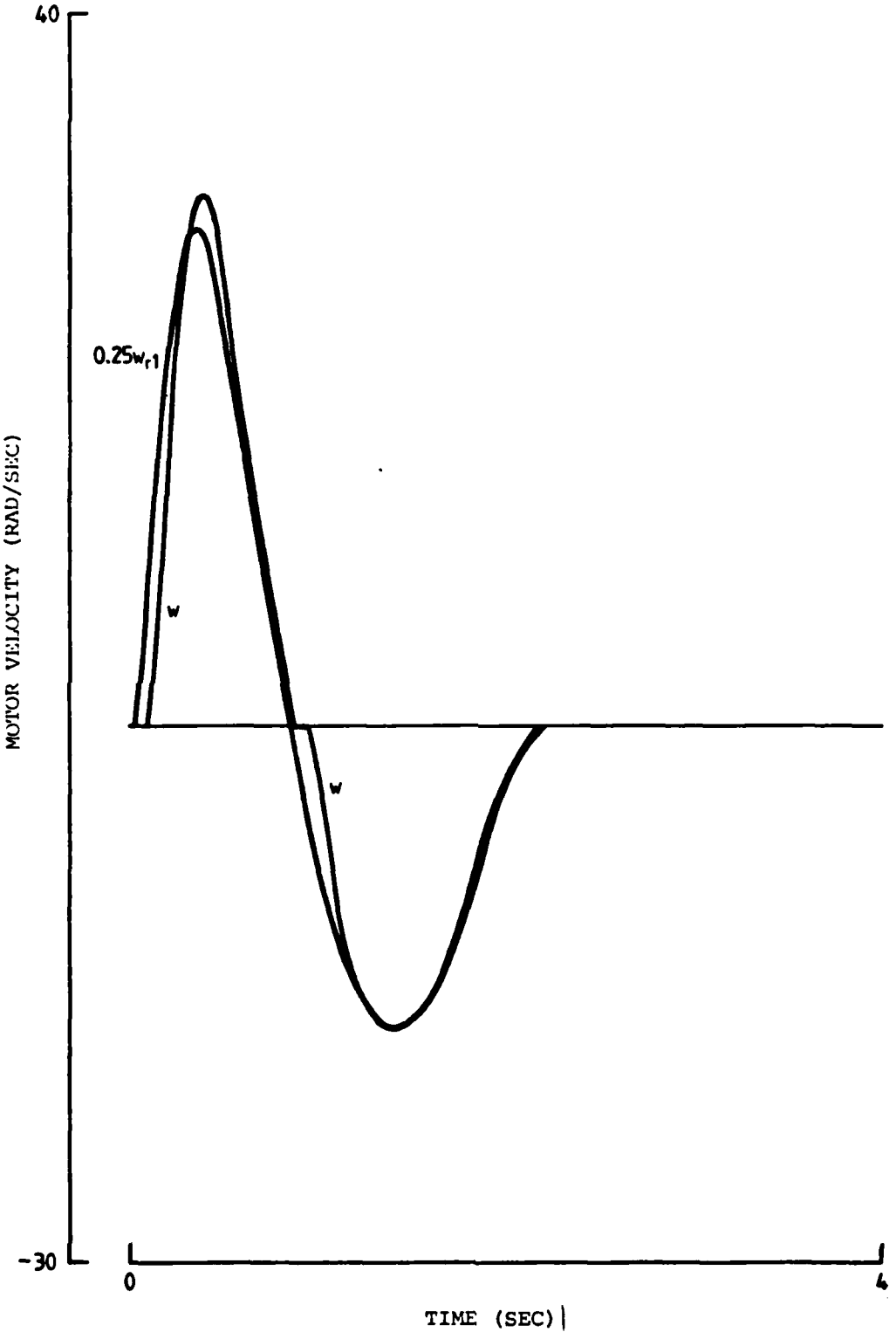

FIG. A1(c) MOTOR RESPONSE TO 0.25 W_{R1}
$J = 4 \times 10^{-3}$ kgm^2, $k_s = 2.5 \times 10^{-2}$ N/m

APPENDIX 1

SIMULATION RESULTS

TABLE A1

Performance Measures From Simulation

REFERENCE INPUT FUNCTION	INERTIA (kg m²)	SPRING RATE (N/m)	$\ell\Delta t$ (msec)	R_w	$R_{\dot{w}}$
w_{r1}	4×10^{-3}	2.5×10^{-2}	40	0.07	0.20
w_{r2}	4×10^{-3}	2.5×10^{-2}	60	0.08	0.27
$0.25\ w_{r1}$	4×10^{-3}	2.5×10^{-2}	60	0.10	0.34
w_{r1}	2×10^{-3}	2.5×10^{-2}	40	0.05	0.29
w_{r2}	2×10^{-3}	2.5×10^{-2}	40	0.06	0.43
$0.25\ w_{r1}$	2×10^{-3}	2.5×10^{-2}	40	0.09	0.59
w_{r1}	6×10^{-3}	2.5×10^{-2}	60	0.12	0.28
w_{r2}	6×10^{-3}	2.5×10^{-2}	60	0.12	0.33
$0.25\ w_{r1}$	6×10^{-3}	2.5x10-2	60	0.10	0.35
w_{r1}	4×10^{-3}	0	40	0.10	0.35
w_{r2}	4×10^{-3}	0	60	0.08	0.26

TABLE A2

Performance Measures for Nonlinear Control

REFERENCE INPUT FUNCTION	INERTIA (kg m²)	SPRING RATE (N/m)	$\ell\Delta t$ (sec)	R_w	$R_{\dot{w}}$
$0.25\ w_{r1}$	4×10^{-3}	2.5×10^{-2}	60	0.9	0.33
$0.25\ w_{r1}$	2×10^{-3}	2.5×10^{-2}	40	0.9	0.53

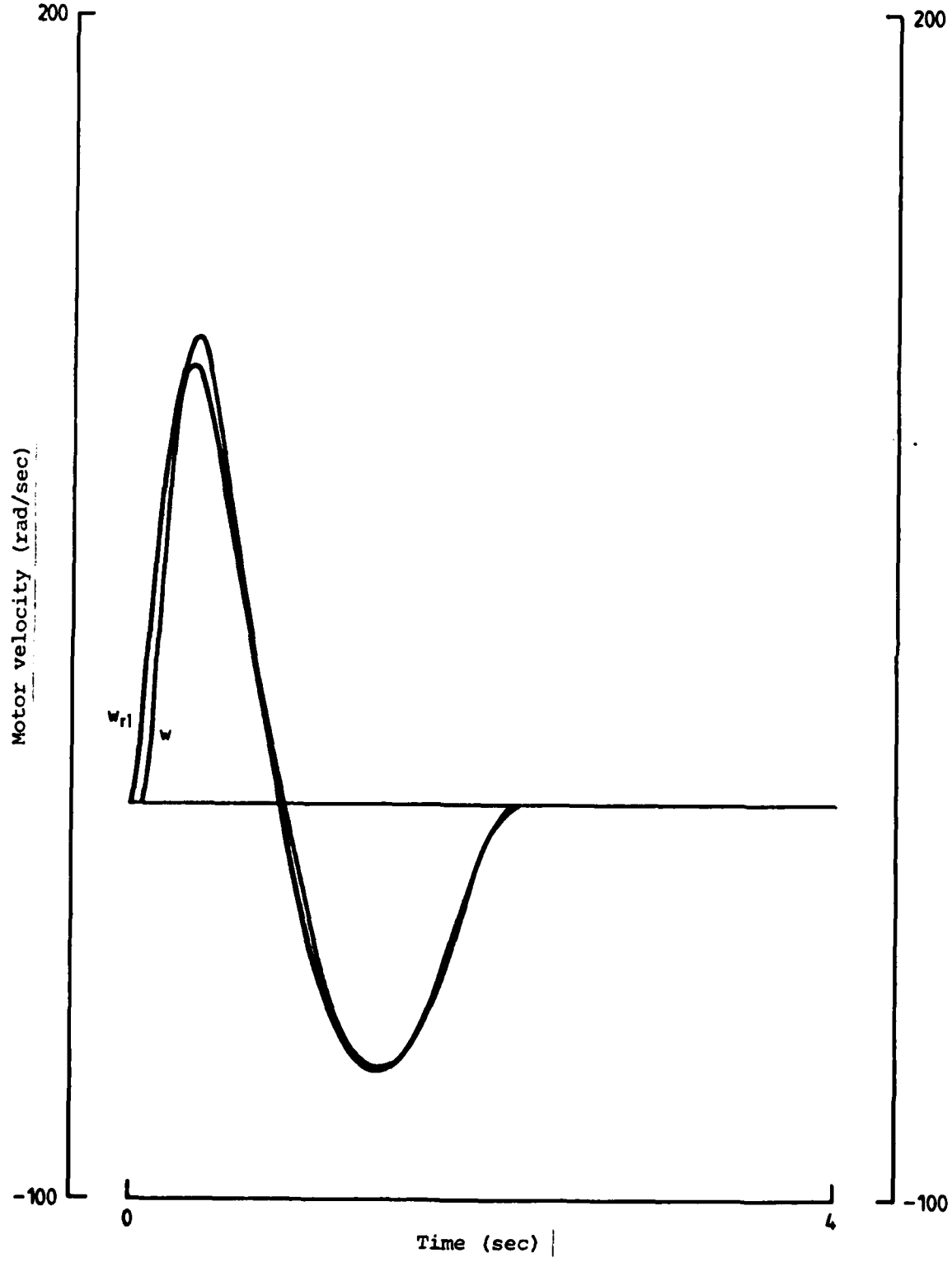

FIG. A1(a) MOTOR RESPONSE TO W_{r1}
$J = 4 \times 10^{-3}$ kgm^2, $k_s = 2.5 \times 10^{-2}$ N/m

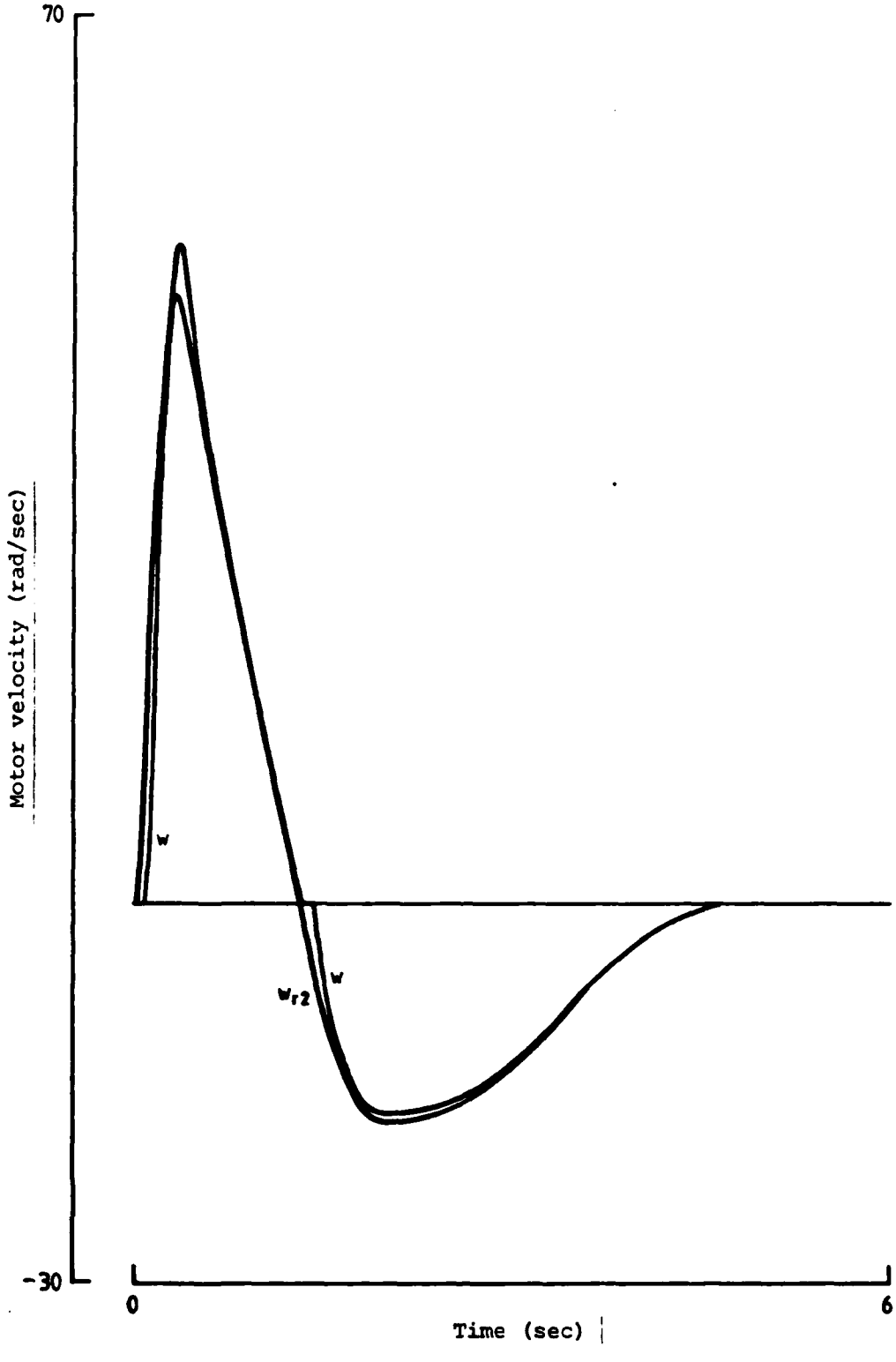

FIG. A1(b) MOTOR RESPONSE TO W_{r2}
$J = 4 \times 10^{-3}$ kgm^2, $k_s = 2.5 \times 10^{-2}$ N/m

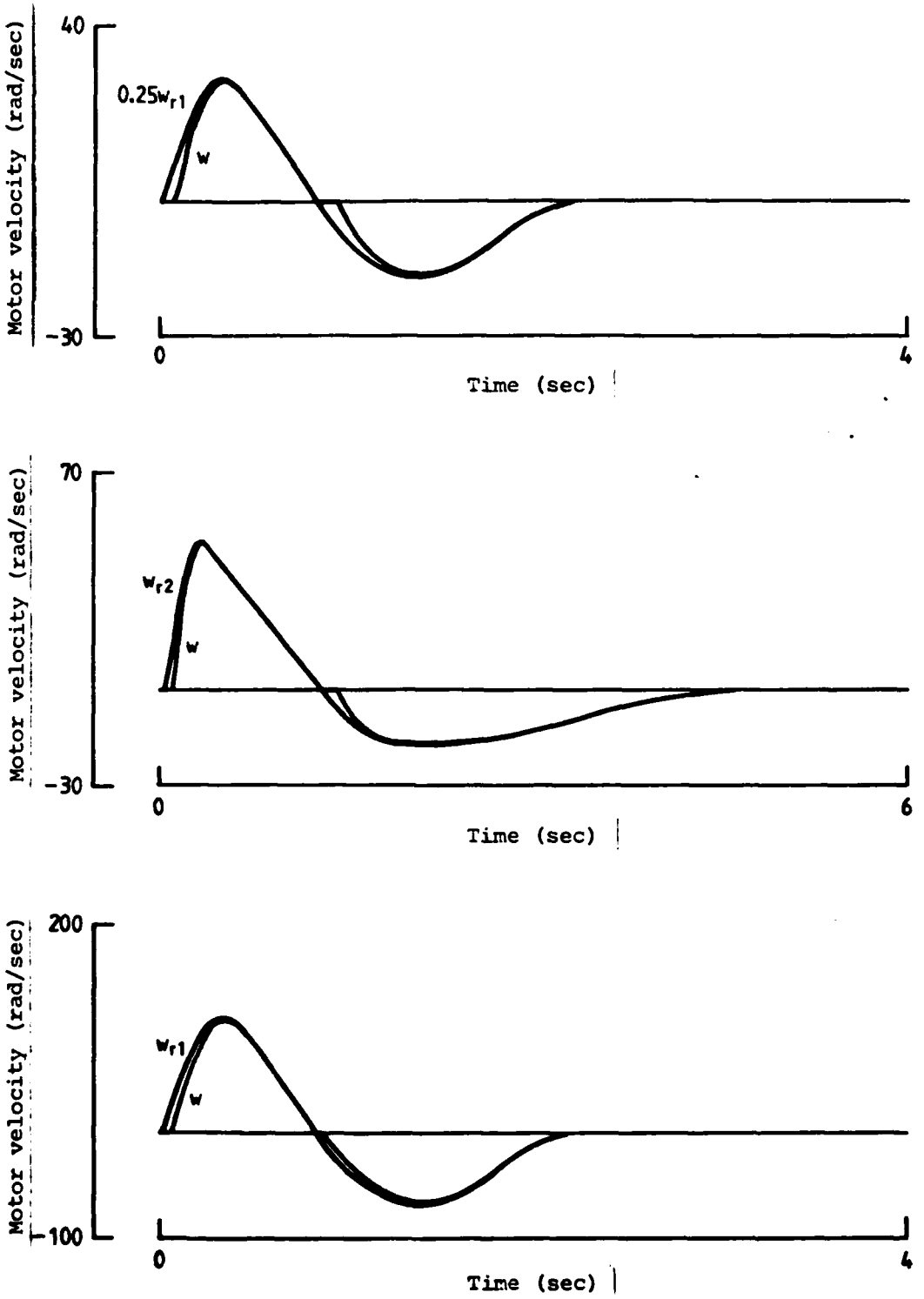

Fig. A1(d) MOTOR RESPONSE
$J = 2 \times 10^{-3}$ kgm^2, $k_s = 2.5 \times 10^{-2}$ N/m

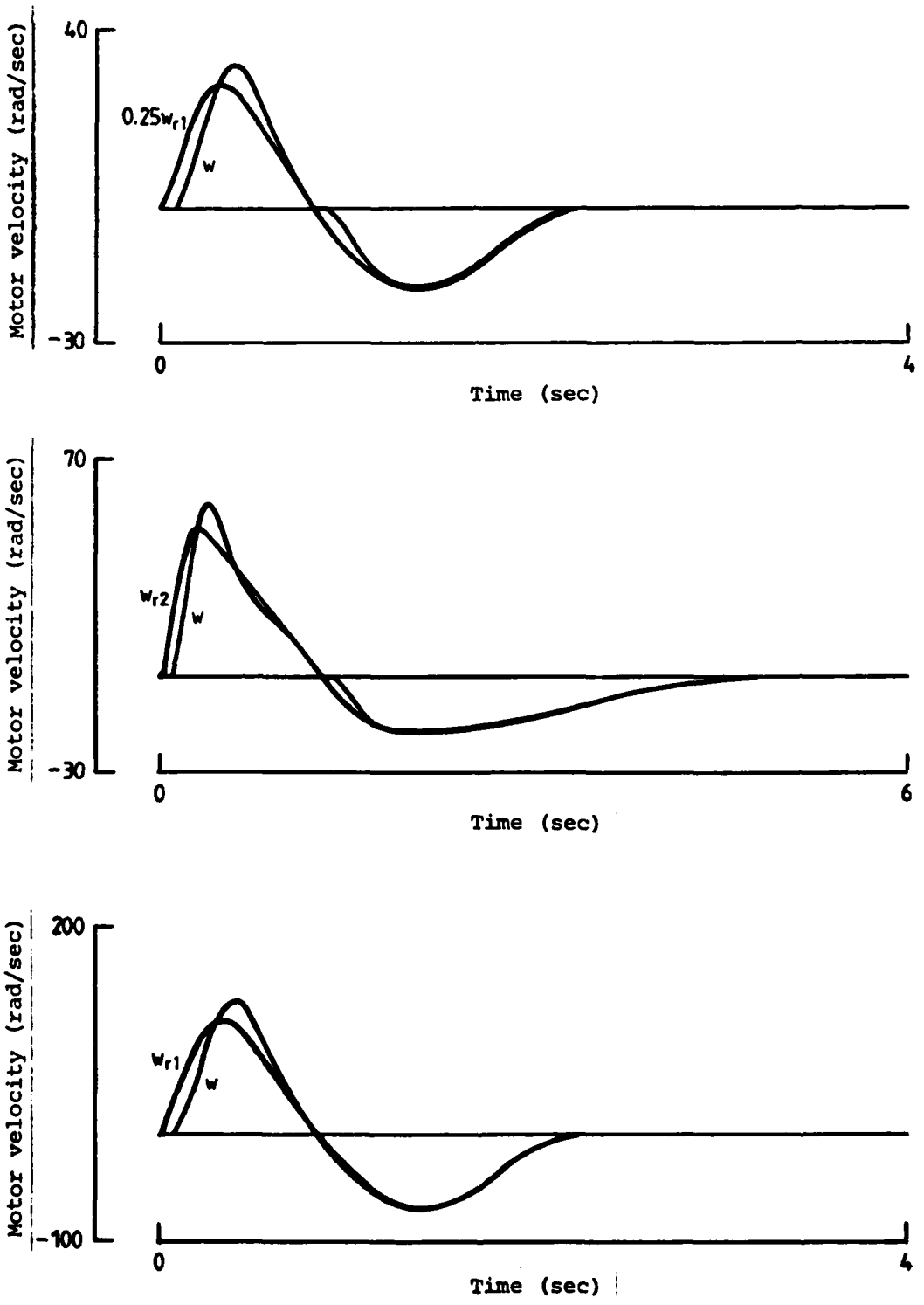

FIG. A1(e) MOTOR RESPONSE
$J = 6 \times 10^{-3}$ kgm^2, $k_s = 2.5 \times 10^{-2}$ N/m

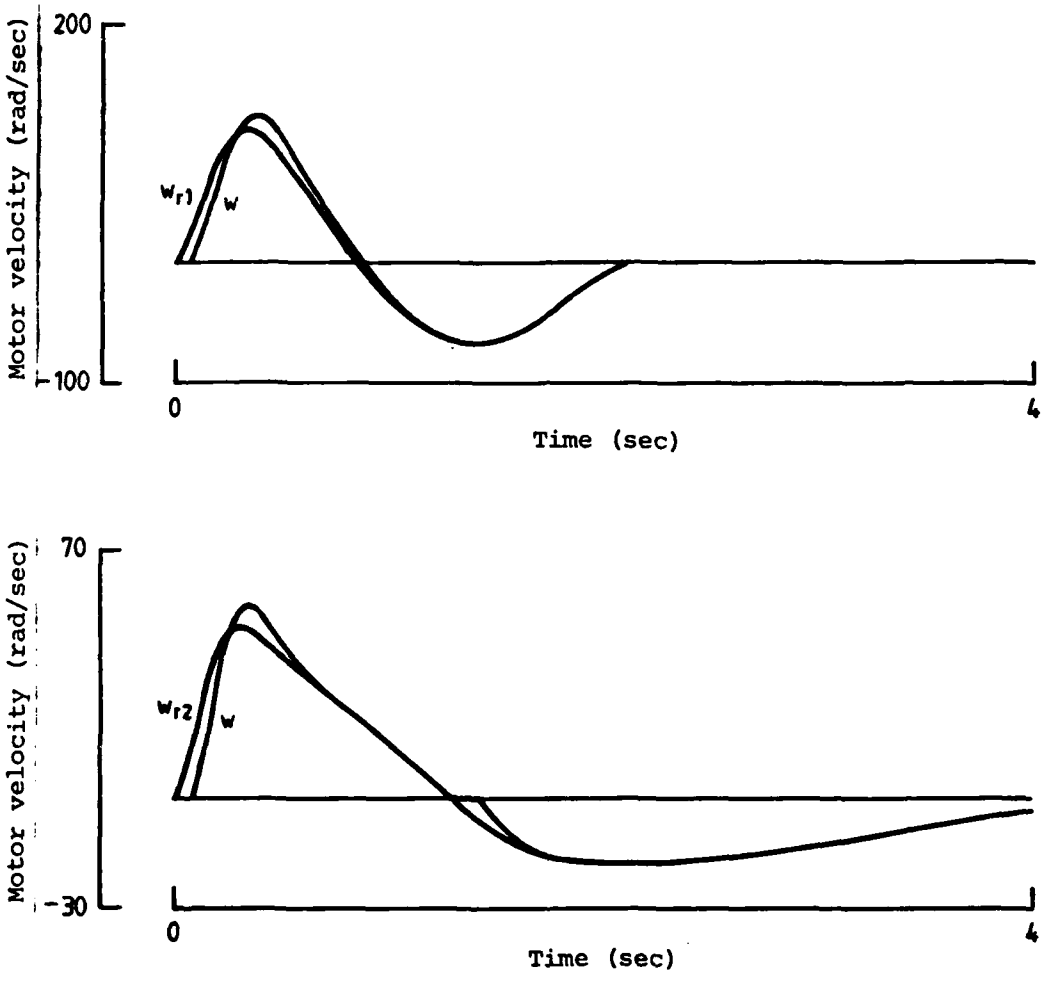

FIG. A1(f) MOTOR RESPONSE
$J = 4 \times 10^{-3}$ kgm^2, $k_s = 0$

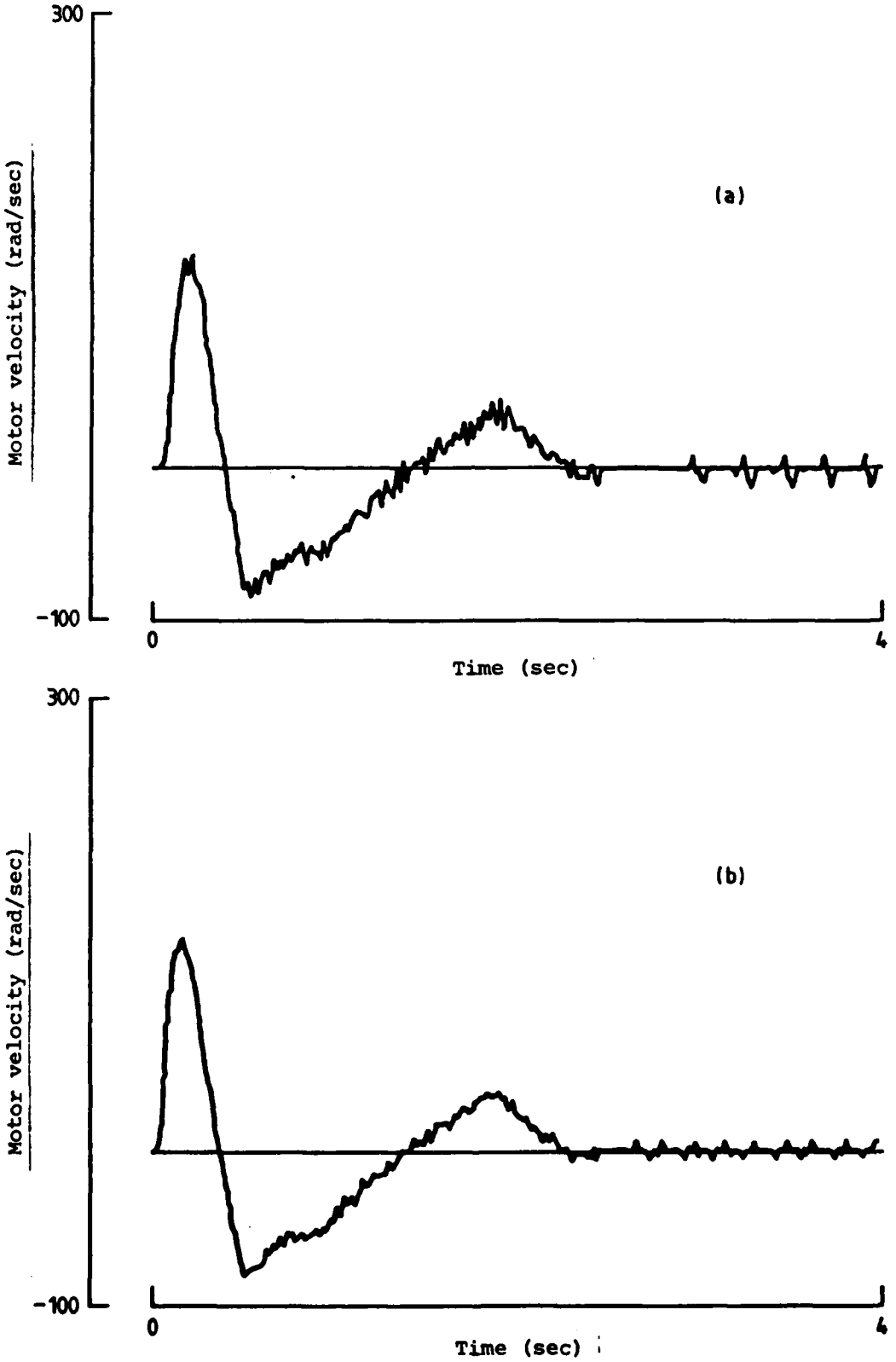

FIG. A2 MOTOR ACCELERATION WITH NO COULOMB FRICTION
$J = 10^{-3}$ kgm $^{-2}$, ks = 2.5 N/m
(a) 600 counts/rev, (b) 1000 counts/rev

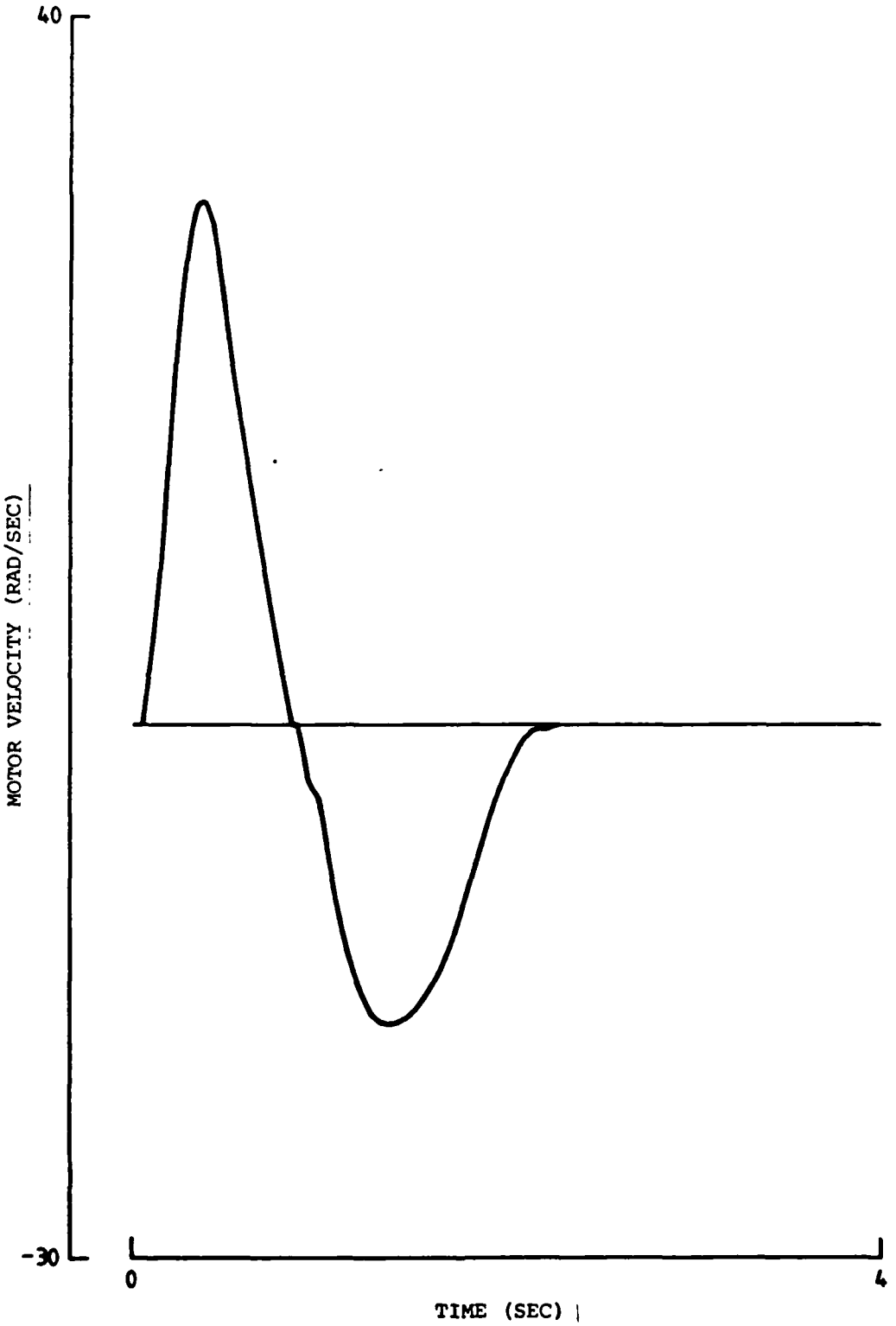

Fig. A2 (CONT)

NONLINEAR CONTROL
MOTOR RESPONSE TO INPUT 0.25 W_{r_1}

$J = 4 \times 10^{-3}$ kgm^2, $ks = 2.5 \times 10^{-2}$ N/m

DISTRIBUTION

AUSTRALIA

Department of Defence

Central Office

Chief Defence Scientist)
Deputy Chief Defence Scientist)
Superintendent, Science and Technology Programmes) (1 copy)
Controller, Projects and Analytical Studies Division)
Defence Science Representative (U.K.) (Doc Data sheet only)
Counsellor, Defence Science (U.S.A.) (Doc Data sheet only)
Defence Central Library
Document Exchange Centre, D.I.S.B. (18 copies)
Joint Intelligence Organisation
Librarian, H Block, Victoria Barracks, Melbourne
Director General - Army Development (NSO) (4 copies)

Aeronautical Research Laboratories

Director
Library
Superintendent Systems
Divisional File - Systems
Author: J. Sandor

Materials Research Laboratories

Director/Library

Defence Research Centre

Library

RAN Research Laboratory

Library

Army Office

Army Scientific Adviser
Engineering Development Establishment, Library

Central Studies Establishment

Information Centre

Department of Defence Support

Government Aircraft Factories

Manager
Library

.../cont.

DISTRIBUTION (CONT.)

Department of Aviation

Library

Statutory & State Authorities and Industry

Trans-Australia Airlines, Library
Qantas Airways Limited, Chief Evaluation Engineer
Ansett Airlines of Australia, Library

Universities and Colleges

Sydney	Engineering Library
N.S.W.	Physical Sciences Library

CANADA
International Civil Aviation Organization, Library

NRC
National Aeronautical Establishment, Library
Aeronautical & Mechanical Engineering Library

INDIA
National Aeronautical Laboratory, Information Centre

ISRAEL
Technion-Israel Institute of Technology
Professor J. Singer

JAPAN
National Aerospace Laboratory
Institute of Space and Astronautical Science, Library

NETHERLANDS
National Aerospace Laboratory [NLR], Library

NEW ZEALAND
Defence Scientific Establishment, Library

SWEDEN
Aeronautical Research Institute, Library

UNITED KINGDOM
CAARC, Secretary
Royal Aircraft Establishment
Farnborough, Library
Admiralty Marine Technology Establishment
Holton Heath, Dr N.J. Wadsworth

Universities and Colleges

Cranfield Inst. of Technology, Library

.../cont.

DISTRIBUTION (CONT.)

UNITED STATES OF AMERICA
NASA Scientific and Technical Information Facility
Boeing Commercial Airplane Co., Library
McDonnell Aircraft Company, Library

SPARES (10 copies)

TOTAL (72 copies)

Department of Defence

DOCUMENT CONTROL DATA

1. a. AR No	1. b. Establishment No	2. Document Date	3. Task No
AR-003-006	ARL-SYS-TM-69	January 1984	DST 82/068

4. Title	5. Security a. document	6. No Pages
DIGITAL CONTROL OF FLIGHT SIMULATOR MOTION BASE ACTUATOR	UNCLASSIFIED b. title c. abstract U U	51 7. No Refs 13

8. Author(s)	9. Downgrading Instructions
J. SANDOR	

10. Corporate Author and Address	11. Authority (as appropriate)
Aeronautical Research Laboratories, P.O. Box 4331, MELBOURNE, VIC. 3001	a. Sponsor b. Security c. Downgrading d. Approval

12. Secondary Distribution (of this document)

Approved for Public Release.

Overseas enquirers outside stated limitations should be referred through ASDIS, Defence Information Services Branch, Department of Defence, Campbell Park, CANBERRA ACT 2601

13. a. This document may be ANNOUNCED in catalogues and awareness services available to ...

No Limitations.

13. b. Citation for other purposes (ie casual announcement) may be (select) unrestricted(or) as for 13 a.

14. Descriptors	15. COSATI Group
Flight simulators Stability criteria Computer applications Control	14020 12010

16. Abstract

Digital control strategies for a nonlinear motion base actuator are considered and a compound linear/nonlinear algorithm is derived for velocity tracking under a range of load conditions for representative motion demands. Discrete frequency domain methods are employed to synthesize the linear components of the control law and to establish the stability of the closed loop system via describing function analysis. The nonlinear compensation, providing attenuation of Coulomb friction effects, is realised through a velocity dependent gain term, which does not significantly affect the satisfactory large amplitude system response. Overall closed loop system performance is validated through computer simulation.

This page is to be used to record information which is required by the Establishment for its own use but which will not be added to the DISTIS data base unless specifically requested.

16. Abstract *(Cover)*

17. Imprint

Aeronautical Research Laboratories, Melbourne.

18. Document Series and Number	19. Cost Code	20. Type of Report and Period Covered
Systems Technical Memorandum 69	71 6490	

21. Computer Programs Used

22. Establishment File Ref(s)

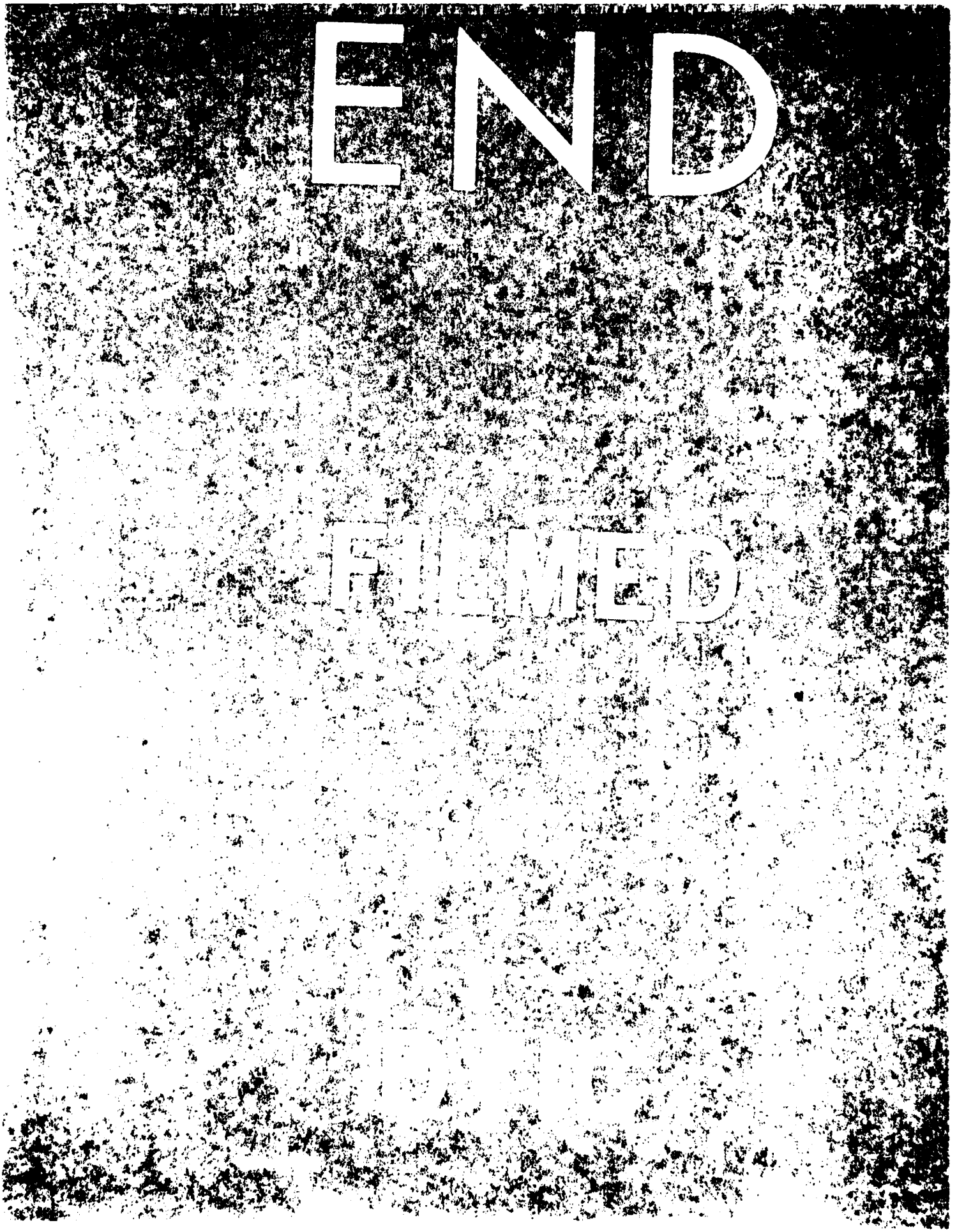
END
FILMED